

**EUR 4196 e**

**EUROPEAN ATOMIC ENERGY COMMUNITY - EURATOM**

**AN IRRADIATION FACILITY FOR IN-PILE MEASUREMENTS OF  
ELECTRICAL RESISTIVITY AT HIGHER TEMPERATURES UNDER  
VARIOUS NEUTRON FLUXES FOR OPTIONAL PERIODS**

by

**E. LANG and W. SCHÜLE**

**1968**



**Joint Nuclear Research Center  
Ispra Establishment - Italy**

**Chemistry Department  
Solid State Physics**

## LEGAL NOTICE

This document was prepared under the sponsorship of the Commission of the European Communities.

Neither the Commission of the European Communities, its contractors nor any person acting on their behalf :

Make any warranty or representation, express or implied, with respect to the accuracy, completeness, or usefulness of the information contained in this document, or that the use of any information, apparatus, method, or process disclosed in this document may not infringe privately owned rights; or

Assume any liability with respect to the use of, or for damages resulting from the use of any information, apparatus, method or process disclosed in this document.

This report is on sale at the addresses listed on cover page 4

at the price of FF 8.50	FB 85.-	DM 6.80	Lit. 1060	Fl. 6.20
-------------------------	---------	---------	-----------	----------

**When ordering, please quote the EUR number and the title, which are indicated on the cover of each report.**

Printed by SMEETS  
Brussels, November 1968

This document was reproduced on the basis of the best available copy.

**EUR 4196 e**

AN IRRADIATION FACILITY FOR IN-PILE MEASUREMENTS OF ELECTRICAL RESISTIVITY AT HIGHER TEMPERATURES UNDER VARIOUS NEUTRON FLUXES FOR OPTIONAL PERIODS  
by E. LANG and W. SCHÜLE

European Atomic Energy Community - EURATOM  
Joint Nuclear Research Center - Ispra Establishment (Italy)  
Chemistry Department - Solid State Physics  
Luxembourg, November 1968 - 52 Pages - 18 Figures - FB 85

An irradiation facility installed at Ispra-I reactor for in-pile measurements of electrical resistivity of fissile and non-fissile material is described.

Samples are brought within capsules into the facility and can be irradiated at temperatures between 40 and 1000°C at positions of different

**EUR 4196 e**

AN IRRADIATION FACILITY FOR IN-PILE MEASUREMENTS OF ELECTRICAL RESISTIVITY AT HIGHER TEMPERATURES UNDER VARIOUS NEUTRON FLUXES FOR OPTIONAL PERIODS  
by E. LANG and W. SCHÜLE

European Atomic Energy Community - EURATOM  
Joint Nuclear Research Center - Ispra Establishment (Italy)  
Chemistry Department - Solid State Physics  
Luxembourg, November 1968 - 52 Pages - 18 Figures - FB 85

An irradiation facility installed at Ispra-I reactor for in-pile measurements of electrical resistivity of fissile and non-fissile material is described.

Samples are brought within capsules into the facility and can be irradiated at temperatures between 40 and 1000°C at positions of different

neutron fluxes for optional periods. Insertion and extraction of capsules can be performed without shut-down of the reactor. A detailed discussion of the shielding calculations is included. Measurements of the neutron flux and distribution inside the facility have been performed. First operation experiences and some irradiation experiments on  $\alpha$ -brass are briefly reported.

neutron fluxes for optional periods. Insertion and extraction of capsules can be performed without shut-down of the reactor. A detailed discussion of the shielding calculations is included. Measurements of the neutron flux and distribution inside the facility have been performed. First operation experiences and some irradiation experiments on  $\alpha$ -brass are briefly reported.

**EUR 4196 e**

**EUROPEAN ATOMIC ENERGY COMMUNITY - EURATOM**

**AN IRRADIATION FACILITY FOR IN-PILE MEASUREMENTS OF  
ELECTRICAL RESISTIVITY AT HIGHER TEMPERATURES UNDER  
VARIOUS NEUTRON FLUXES FOR OPTIONAL PERIODS**

by

**E. LANG and W. SCHÜLE**

**1968**



**Joint Nuclear Research Center  
Ispra Establishment - Italy**

**Chemistry Department  
Solid State Physics**

## SUMMARY

An irradiation facility installed at Ispra-I reactor for in-pile measurements of electrical resistivity of fissile and non-fissile material is described.

Samples are brought within capsules into the facility and can be irradiated at temperatures between 40 and 1000°C at positions of different neutron fluxes for optional periods. Insertion and extraction of capsules can be performed without shut-down of the reactor. A detailed discussion of the shielding calculations is included. Measurements of the neutron flux and distribution inside the facility have been performed. First operation experiences and some irradiation experiments on  $\alpha$ -brass are briefly reported.

## KEYWORDS

ISPRA-I  
IRRADIATION  
IN-PILE LOOPS  
ELECTRIC CONDUCTIVITY  
CAPSULES  
TEMPERATURE  
NEUTRON FLUX  
SHIELDING  
BRASS

Contents:

	<u>page</u>
1. Introduction	1
2. Description of the irradiation facility	2
2.1. - Reactor and beam hole available for the irradiation facility	2
2.2. - Irradiation facility	3
2.3. - Safety installations	5
3. Capsules and specimenholder	7
4. Extraction facility	8
5. Equipment for resistivity measurements	9
6. Performance of experiments	10
7. Neutron flux measurements	12
8. First results and experiences	16
9. References	18
10. Appendix - Calculation of the radiation shielding for the irradiation facility	19
10.1. - Shielding efficiency of a tube in spiral form	19
10.1.1. Neutrons directly scattered through the tube	19
10.1.2. Neutrons penetrating the shielding materials	21
10.2. - Additional shielding and total dose rate	23
10.3. - Radiation resistance of polyethylene	25
11. List of Figure Captions	26
Table 1	28





## 1. INTRODUCTION

During the past years measurements of changes of physical properties due to irradiation in nuclear reactors has become important for the technological development of reactor materials as well as for fundamental research on solids at all.

Irradiations can be executed in two classes of experimental facilities: capsules or loops. In capsules heat transfer takes place by conduction and radiation whereas in loops convection cooling by recirculating a gas or liquid is employed. This requires circulation pumps. Schematically this is demonstrated by Fig. 1.

Capsules are simple and cheaper to design and build; therefore they can be developed for single use only, providing thus the advantage of easy substitution in case of experiment failure. Moreover capsule experiments can be performed on shorter time schedules than loop experiments. As a result, capsule experiments have become increasingly popular.

Measurements of physical properties, such as mechanical strength, density, thermal diffusivity or conductivity, electrical resistivity, (thermal EMF) thermoelectric power etc. can be made in pile or after removal of a sample from the reactor. The electrical resistivity is the most commonly investigated parameter due to the simplicity of required experimental technique and high accuracy of results.

Though requiring a larger effort and needing a higher precision of measuring equipment, in-pile measurements have the advantage that no extraction is needed and there is no need to await decay of activity of the irradiated sample.

For these reasons it was decided to construct an in-pile capsule facility for irradiation and measurement of the physical properties mentioned. We designed this facility for the Ispra-I reactor, to operate above room temperature <sup>\*</sup>) and to provide for the possibility of inserting and extracting samples

---

<sup>\*</sup>) A low temperature irradiation facility (to  $-190^{\circ}\text{C}$ ) in the 4GV1 beam of Ispra-I reactor has been taken into operation during 1966, see ref. (2).

without necessity of a shut-down of the reactor and also to provide for irradiations at positions of different neutron fluxes. The capsule facility herein described fulfills these conditions.

## 2. DESCRIPTION OF THE IRRADIATION FACILITY

### 2.1. Reactor and beam hole available for the irradiation facility

The irradiation facility has been installed in the 4DH3 beam of Ispra-I reactor of the Joint Nuclear Research Center, Ispra, Italy (EURATOM). Fig. 2 shows a cross-sectional view of the reactor with the position of the various beam holes for irradiation experiments.

The Ispra-I reactor is a heavy-water cooled and moderated experimental reactor of type CP 5. Its maximal thermal power amounts to 5 MW. The reactor is operated with enriched uranium (90% U-235). The active core consisting of 18 fuel elements of type MTR and 6 control rods is enclosed by a heavy-water container made of aluminium.

The reflector is partly formed by heavy-water (top and bottom), partly by a cylindrical mantle of nuclear graphite (type AGOT). The thermal screening is made of a 5 cm thick Boral cylinder and two cylinders of stainless steel between which cooling water is circulated in order to carry off 90% of the gamma heating of the fission products. The biological shielding is provided by a 1.80 m thick mantle of reinforced concrete ( $\rho = 4.5 \text{ g/cm}^3$ ). The dose rate at the reactor wall is approx. 1 mrem/h at 5 MW reactor power.

The maximum neutron flux in the reactor core amounts to  $4.6 \times 10^{13} \text{ n/cm}^2 \text{ sec}$ , the corresponding thermal neutron flux being  $1.4 \times 10^{13} \text{ n/cm}^2 \text{ sec}$ . The neutron flux in the experimental beam holes depends to some extent on how the 18 fuel elements are distributed among the 29 possible fuel element locations in the core.

The horizontal radial channel 4DH3 in which the facility had to be installed is indicated in Fig. 2. The beam hole is divided into three parts; the inner section consists of an aluminium tube, reaching from the thermal screening almost to the heavy-water container.

The core-side end of the hole is distant about 65 cm from the center of the core. The middle section is a stainless steel tube leading through the concrete mantle of the biological shield and ending with a rectangular box which contains the fittings for the cooling water, electrical power supply and a junction canal for the air recirculation system. Beam holes not being occupied by loops or facilities are normally closed by plugs to keep the dose rate at the reactor wall at 1 mrem/h. These plugs have the form of the middle and inner section of the beam tube and consist of a stainless steel tube filled with baryth concrete, connected to a smaller aluminium tube containing lead and Boral. Such a plug has been substituted in the 4DH3 beam hole by the irradiation facility described in the next paragraph.

## 2.2. Irradiation Facility

Fig. 3 is a schematic drawing of the irradiation facility in hole 4DH3. The apparatus has the external dimensions of the plug retracted from hole 4DH3 and is constructed of stainless steel for mechanical and thermal stability. It may be divided into two parts; the outer thicker section ( $\phi$  20 cm, length 1.30 m) forms the shield, whereas the reduced inner part ( $\phi$  10 cm, length 80 cm) is the proper irradiation facility. An O-ring seal at the outer end of the plug prevents the release of radioactive gas from the beam hole into the reactor hall.

The samples to be irradiated are inserted within capsules into the so-called sample chamber - a stainless steel tube of 5.7 cm diameter spiralling through the shield into the irradiation section. The sample tube - as well as all other tubings (see below) - in passing through the shielding plug makes a full ( $180^\circ$ ) spiral line, so that on any straight line the not-shielded distance does not exceed 30 cm. This spiral tube provides for insertion of capsules to suitable irradiation positions and their extraction from the facility without shut-down of the reactor.

The sample chamber is getting closed vacuum-tightly by a fast connected bayonet flange (see Fig. 4) containing several feed-throughs for the leads running to the capsule.

The temperature of the graphite near the core approaches  $280^\circ\text{C}$ , decreas-

ing outside the thermal screen. For example at a distance of 80 cm, it is about  $120^{\circ}\text{C}$ . In order to carry off the nuclear heat arising from gamma-heating and fast neutron scattering in the structure materials of the apparatus and also in order to permit performance of irradiation experiments at lower temperatures (approx.  $40^{\circ}\text{C}$ , temperature of cooling water), at the core-side part of the facility a water cooling circuit is included as shown in Fig. 3. This cooling system is supplied with demineralized water available from the reactor system.

If the cooling water entering the line which is passed through a thermostated refrigerator ( $+20$  to  $-80^{\circ}\text{C}$ ,  $1400$  kcal/h) which may be located outside the beam hole, then the irradiation facility can be used for irradiating normal samples below room temperature or for irradiating fissile materials which produce a lot of fissile heat. The water lines are also made of stainless steel and run in a spiral through the shield.

Shielding calculations performed, reproduced in detail in the Appendix have yielded the following results: The lesser shielding thickness of the radiation facility can be largely compensated by using more efficient shielding materials. Instead of baryth concrete as used in the blind plug, the radiation screen of the facility consists (from inside to outside) of a 5 mm thick layer of Boral, 10 cm lead followed by a reinforced concrete (Schwerbeton) layer ( $\rho = 4.8$  g/cm<sup>3</sup>) of 52 cm thickness and another 3 cm thick plate of Boral and finally a polyethylene<sup>+</sup> packing of 60 cm. This results in a neutron dose rate at the end of the facility of 7 mrem/h. Additional shielding has been achieved by filling the junction box (see Fig. 3) with polyethylene and lead. This junction box had been empty when the blind plug was inserted. The calculations show that 20 cm of polyethylene should improve the shielding by a factor 10.

For shielding against the gamma radiation resulting from (n,  $\gamma$ )-capture processes in the iron of the concrete, a 20 cm thick wall of lead bricks was

---

<sup>+</sup>) The reinforced concrete consists of a mixture of small iron pieces (70%), iron powder and filings (17%), cement (9%) and water (4%) - a mixture almost corresponding to a concrete described in ANL 5800. The water not bound after the concrete has grown stiff, was driven out by heating the facility. The polyethylene layer ( $\rho = 0.9$  g/cm<sup>3</sup>) was produced by successive melting of granulated material ( $\rho = 0.54$  g/cm<sup>3</sup>) inside the facility.

built behind the last polyethylene layer. The dose rate finally measured after installation of the facility in the reactor amounted to about 2 mrem/h at the entrance of the sample tube, demonstrating good agreement with the calculations performed before.

### 2.3. Safety Installations

Several safety devices for the cooling, vacuum and heating system, respectively, had to be installed, (see Fig. 5, 6).

#### a) Cooling water system:

Due to the fact that the facility is constructed of bad heat conducting material, the heat generated in the material by radiation and nuclear heat has to be carried off by an external cooling system. Previous measurements by BASSANI and CERUTTI (3) indicated that at 5 MW reactor power in 1 g material approx. 0.06 Watt are produced by gamma heat generation. Calculations have shown, that in our case the gamma heat contribution amounts to approx. 500 Watts, whereas heat conduction and radiation produce about 200 Watts, i. e. the total heat generated in the part of the facility to be cooled (front part of the facility) amounts to approx. 700 Watts. Heat removal by conduction and convection being neglected, the cooling water circuit has to lead off approx. 170 cal/sec. With a minimum water flow of 3 l/min the outlet temperature of the water is about 4°C higher than that at the inlet. Normally the flow was higher (5 l/min) and we had no difficulties carrying off heat even with heated capsules inside the sample chamber.

The efficiency of the cooling system is monitored by thermocouples attached to several points inside the facility and their output is continuously recorded. The inlet and outlet temperatures of the cooling water are measured with Thermocoax thermocouples soldered into the water lines. If these thermocouples indicate a temperature rise of the cooling water over a certain critical value, a controller will cause the sample heating current to be turned off and a light to go on at the experimenter's console. This series of events will also occur when the water flow rate measured by a pressostat and a flowmeter drops below a set minimum value. Flow and pressure of water are also monitored on indicating instruments. The cooling water may be stopped manually by an electromagnetic valve, which

can also be set to operate automatically in case of a failure in the vacuum jacket due to leakage of the internal water circuit. Such a leakage is also monitored by the pressostat and/or the thermocouples (acting as leak detectors), which close the water valve and switch off the heater current via a relay.

Further a safety relief valve is installed venting the internal cooling system in case of accidental excess pressure in the water piping (> 3 ata) caused, for example, by boiling inside the facility. The water entering the system is demineralized and running through fine sieves to prevent clogging of the cooling coil.

b) Vacuum system:

Fig. 5 shows schematically how the two vacuum systems of the installation are controlled.

i. The function of the vacuum-jacket at the front section of the facility has been already described above. A failure of the vacuum measured by a Thermotron and a Penning gauge causes a Torrostat to produce alarm signals, to stop the entrance of cooling water, and to switch off the heater current. Evacuation is performed by means of a rotary- and an oil-diffusion-pump equipped with a cold trap and achieving a vacuum of better than  $1 \times 10^{-5}$  Torr. Electromagnetic and -pneumatic valves are operated from a central switchboard. A pressure relief valve protects the facility against excess pressure. The response of the vacuum gauges is continuously recorded.

ii. The sample tube system is similarly equipped (see Fig. 5) and is used for evacuation of the sample chamber and also for filling it with inert gas (He). Fission gas, released by accident from a capsule will be captured at a gas trap cooled by liquid nitrogen. Moreover, to prevent any contamination, all exhausts of pumps, relief valves, vacuum cleaners etc. are sent via special filters to the reactor off-gas system; also the oil of the pumps is acting as a filter for solid (radioactive) particles. The filters can be continuously monitored by a HERFURTH-gamma-ray monitor which triggers an alarm if the radioactivity of a filter reaches a preset level.

c) Heating System and Electric Power Supply:

The desired specimen temperature is achieved and regulated by an elec-

tric resistance heater inside each capsule (see par. 3, Fig. 8, 10). Fig. 6 shows the safety devices installed for controlling the heater current. In case of interruption of electric power, our equipment (3 KW) is automatically connected to the reactor emergency power supply.

Fig. 7 shows a view of the vacuum and control equipment and auxiliary apparatus in front of the irradiation hole 4DH3.

### 3. Capsules and specimenholder

Two types of capsules have been developed:

i. Capsule for irradiation of non-fissile material at medium temperatures (up to  $400^{\circ}\text{C}$ ). Some capsules of this type are shown in Fig. 8. They consist of pure aluminium (ANET), 1 mm thick, total length being 12.5 cm, diameter 4.5 cm, weight approx. 100 g. The holes are provided for good evacuation via sample tube and/or for sufficient heat transfer (from the specimen to the cooling coil) by the inert gas (He).

The heater for this capsule type was made of an asbestos and silica isolated NiCr-wire ( $\emptyset$  0.1 mm, 220 cm), wound on a 1 mm thick cylinder of ANET fitting properly into the capsule. The resistor wires are hard soldered onto copper leads running via the bayonet flange to the regulated current supply (see Fig. 14). The specimenholder is introduced between two guides fixed at the heater cylinder. The holder itself is made of ERGAN (49.5% MgO % 48.6% SiO<sub>2</sub>) or of pure Al<sub>2</sub>O<sub>3</sub>. The specimen is mounted between small stainless steel plates (see Fig. 9) to which the current and tension leads are hard soldered. It is important to mount the two tension probes as near together as possible to prevent (high) thermal voltages produced by temperature gradients.

The capsule contains three thermocouples. They are fixed with springs or - in case of metallic foils - are welded by a condensator discharge onto the specimen; two of them serve for measuring the proper sample temperature, the third one is used for heater current regulation via a temperature controller.

The specimenholder described above can also be easily modified for simultaneous experiments with several (2-3) samples. These samples would be irradiated with neutron fluxes that differ only slightly.

ii. For temperatures higher than  $400^{\circ}\text{C}$  (up to  $900^{\circ}\text{C}$ ) the capsule has to be made of Inconel or stainless steel. The heater element for that case consists of a thin inconel tube on which by means of  $\text{Al}_2\text{O}_3$ -spray coating a bare heater band is fixed. The heater is surrounded by two cylindrical radiation shields made of molybdenum.

To prevent temperature gradients along the specimen, the heater support tube has to be of good heat conducting material. For temperature uniformity there are also provided radiation shields at both ends of the heater tube. The same specimenholder as for capsule i) is used.

The high temperature capsule can also be utilized for irradiation of fissile material. However, in that case the capsule cap, containing special feed-throughs for the wires, has to be argon-arc-welded to the capsule body after the specimenholder has been inserted. Through a clamped flange at the opposite end, the capsule may then be evacuated and filled with 400 Torr helium for protection and heat transfer (if necessary). After closing the capsule, pressure (vacuum) tightness at operating temperature must be checked before the fissile material is inserted into the neutron flux. Fig. 10 represents a draft of this capsule type on plain scale.

#### 4. Extraction Facility

Because of the high radiation dose to be expected from irradiated capsules and danger of spread of contamination, a special facility had to be designed for the extraction of irradiated capsules. Fig. 11 shows a schematic draft of the plant. The thickness of the lead shielding is calculated for a reduction of the radiation dose by a factor 100. For extraction operation, the tap of the sample tube is removed and the wires running to the capsule are connected to another wire fixed at the pulley of the extraction facility.

Then the apparatus with open shutter door is pushed over the exit of the sample tube and by rolling up the wire, the capsule becomes withdrawn into the lead container. Having closed the shutter door, the wires at the sample capsule can be cut by means of a wire nippers mechanism.

For transfer operation the lead container is turned by  $90^{\circ}$  around its axis and by help of a special lifting charriot a transfer flask, also made of lead, and provided with a shutter door is put beneath. By opening the two shutters the capsule drops into the transfer container (see Fig. 12).



During the time a capsule stays inside the extraction facility an under-pressure of some centimeters of water is produced by means of a special vacuum cleaner to prevent possible escape of radioactive gas or dust. Remote operation is possible, and we are able to extract and transfer "hot" capsules with little danger of radiation exposure to personnel or of contamination. After substituting the wire pulley with the irradiated wires by a new one, the extraction facility is ready for further operations.

### 5. Equipment for resistivity measurements

The facility was mainly intended for examination of changes of electrical resistivity due to neutron irradiation - a very sensitive indicator for radiation effects especially in alloys.

The sample resistance is determined by measuring at constant current and at a fixed temperature the potential drop along the specimen with a Diesselhorst potentiometer (WOLFF, precision  $\pm 5 \times 10^{-9}$  V). Null detection is provided by a sensitive galvanometer with a photocell amplifier. Thermal EMFs in the measuring circuit are eliminated by commutating the sample current by means of a special thermal-EMF-free commutator (UT 10, WOLFF).

The auxiliary current for all potentiometers used was originally taken from storage batteries, it is now supplied by a GUILDLINE Type 8780 DC-constant voltage source in order to achieve a more service-free operation of the instrumentation.

To keep constant the sample current, an automatic constant current controller has been developed, regulating the current at 1 A with a precision of 1 ppm. Its principle (see Fig. 13) is the following: The potential drop of the sample current along a standard resistor (1 Ohm) is compared with the nominal value (f. e. 1,000,000 V) fixed by a TINSLEY potentiometer. The actual deviation indicated by the null detection-galvanometer operates on a movable photocell (Photozellen-Nachlaufschreiber, LANGE) following the galvanometer's light spot. This photocell is acting as a switch by which - via relay - motors connected to resistors are operated. These motors vary the resistance of the fine current regulation until the deflection of the galvanometer is again at zero position. Optical and acoustical alarm signals become active if the fine regulation range is exceeded and the coarse regulation in form of a variable resistor combination has to be utilized. By

switching-in fixed resistors the plant can be easily extended to currents up to 10 A.

The sample current previously also taken from storage batteries is now provided by a regulated (0.01%) constant current unit (HEWLETT-PACKER).

As reference voltage for the various potentiometers (for voltage and temperature measurements and current controller) Eppley-Weston Cells are used. Being installed in a temperature controlled box ( $31.8 \pm 0.01^\circ\text{C}$ ) their reference voltage (1.018006 V) has a long time stability of  $\pm 0.4 \mu\text{V}$ . The Diesselhorst potentiometer and the reference standard resistors are kept in a well isolated oil bath, the temperature of which is maintained at  $20^\circ\text{C}$  ( $\pm 0.1^\circ\text{C}$ ) by recirculating the oil through an external thermostat (COLORA). Thus the temperature changes of the surroundings (reactor hall) being normally as high as  $8^\circ\text{C}$  in 24 hours do not influence the precision and calibration of the measuring equipment.

The specimen temperature is measured by two thermocouples and regulated by one thermocouple which are attached at the sample. These and all other control thermocouples (see 2.2) are connected by special thermal EMF-free connectors (LEEDS and NORTHRUP) to extension cables running from the exit of hole 4DH3 to the measuring desk.

The reference temperature ( $0^\circ\text{C}$ ) for all thermocouples is provided by a water-ice reference chamber (FRIGISTOR) with a precision of  $\pm 0.05^\circ\text{C}$  and a long time stability of  $0.01^\circ\text{C}$ . Temperatures are determined by a potentiometer with a precision of  $\pm 0.02^\circ\text{C}$ .

All equipment for the measurements has been installed on a platform in the reactor hall as shown by Fig. 14. Shielded leads and extension cables - 35 meters long - connect the equipment with hole 4DH3.

## 6. Performance of experiments

Irradiation experiments with the facility described in the foregoing are normally performed as follows:

The specimen is mounted on its holder which is then inserted into the capsule. The leads and thermocouples are cut to suitable lengths and are fixed at the bayonet flange. Then two stiff aluminium wires are attached to the cap of the capsule to be used for pushing the capsule into the spiral shaped sample tube. Since jamming of the sample tube would lead to a breakdown

of the experiment, each capsule is first tried out in dummy sample tube before insertion into the reactor. This pre-introduction operation also permits accurate determination of the capsule's irradiation position. Before any chosen irradiation is begun, the sample is brought to the desired irradiation temperature by the electric heater. Having closed the sample chamber, it is evacuated or purged several times with helium (1 ato) in order to achieve good heat transfer as well as an inert atmosphere. The heater power necessary to maintain the sample at any desired temperature in the range from 40 to 400°C at different helium-pressures has been determined by auxiliary experiments. Thus an immediate achievement of the sample equilibrium temperature after insertion of the capsule is possible. During introduction- and extraction operation in hole 4DH3 a vacuum cleaner at the sample tube exit (see Fig. 3) produces a slight underpressure in order to prevent spread of possible contamination from inside the tube into the reactor hall.

After the insertion operation is completed, the sample resistance and simultaneously the sample temperature  $T_p$  are measured. The measured resistance values  $R_p$  can then be related to a nominal temperature  $T_s^*$  by the following equation:

$$R_s = R_p + (T_s - T_p) \times \frac{dR}{dT}$$

The change of resistance with temperature  $\frac{dR}{dT}$  is known or can easily be determined by an auxiliary experiment. With this procedure it is not necessary to keep the irradiation temperature at a perfectly constant value; it may vary slowly within some degrees.

For experiments in which the sample is annealed between irradiations, the capsule is withdrawn while the vacuum cleaner is running, to a position in the biological shield of the reactor (1.10 m from the core-side end of the facility). Annealing in this position permits the original state of the sample (see par. 8) to be reestablished. After that a new experiment at different irradiation temperature or neutron flux can be executed. Final extraction of the capsule is done as described in par. 4.

---

\* $T_s$  being the mean value of all measured temperature values  $T_p$ .

## 7. Neutron flux measurements

It can be supposed that the production of point defects under reactor irradiation is proportional to the fast neutron flux  $\phi_f$

$$K_f \sim \phi_f$$

In addition to point defects produced by direct neutron-atom-collision, there are also produced point defects by  $(n, \gamma)$ -processes; this latter process is especially significant when the sample is in an irradiation position where  $\phi_{th} \gg \phi_f$ . A thermal neutron becomes captured by a lattice atom, gamma rays are emitted which may produce point defects by causing the emitting atom to recoil. This process may be considered to be proportional to the thermal neutron flux,  $\phi_{th}$ .

$$K_{th} \sim \phi_{th}$$

According to COLTMANN et al. (4)  $K_{th}$  may be evaluated from the following relation:

$$K_{th} = \sigma_{th} \phi_{th} \frac{\overline{E_\gamma^2}}{4 M^2 c T_d}$$

where:  $\sigma_{th}$  = thermal neutron cross section

$\overline{E_\gamma^2}$  = weighted mean value of gamma ray energy

$T_d$  = displacement energy

$c$  = velocity of light

$M$  = mass of emitting atom

It is necessary therefore, for a discussion of irradiation experiments and for correlation of results of experiments performed at different neutron flux positions as well as for comparison with data in literature, that both the integrated neutron flux and its energy distribution be well known for all the irradiation positions in hole 4DH3. For this reason neutron flux measurements in the irradiation facility have been performed in collaboration with the Nuclear Chemistry Group of CCR Ispra. Fast neutron flux distribution is commonly determined by threshold detector techniques, whereas epithermal and thermal neutron fluxes are evaluated from  $(n, \gamma)$  activation analysis of suitable detectors. For a detailed discussion of pro-

cedure and mathematical treatment we may refer to the work of DI COLA and ROTA (5, 6) and BRESESTI et al. (7, 8).

In Table 1 the various detector elements and dosimetry parameters used for our neutron flux measurements are listed; Fig. 15 shows the energy spectra of the reaction and thermal capture cross sections of the detectors as used for data evaluation.

All detectors except Mg have been irradiated in metallic form (small disks or wires) of high purity material; Mg has been used in form of MgO enclosed in small glass ampoules. The detector elements were covered for protection against contamination with thin aluminium foils and put into small cadmium containers to prevent activation by thermal neutrons. The samples were positioned in the beam hole by placing them in tiny aluminium containers (ANET) of 1 mm thickness and inserting these in the usual way into the sample tube.

The detectors Co and Au (no. 1 - 4, Tab. 1) were used in determining the thermal and epithermal neutron flux. These monitors were irradiated both bare and enclosed in the 1 mm thick Cd capsule. The Co and Au monitors were irradiated in form of aluminium alloys (Co-Al; 0.099% Co, Au-Al; 0.101% Au) in order to minimize self-shielding effects.

The cut-off energy of the 1 mm thick Cd-shielding was determined to be 0.55 eV. Irradiating under Cd, the activation of Au is produced nearly exclusively by neutrons of the resonance energy of 4.9 eV; whereas the activation of Co is caused predominantly by neutrons of the resonance energy 132 eV.

The irradiations were mainly done at 5 MW reactor power, results of 3.5 MW irradiations showing full correspondence. Irradiation time depended on the position of the containers in the sample tube and was between 30 min. and 5 hours, followed by a  $\pm$  12 hours storage for the decay of radioactivity before counting could be started.

Flux measurements were performed at several positions along a 70 cm distance from the core-side end of the facility (see Fig. 17).

Activation analysis was performed by gamma counting utilizing a gamma spectrometer which consisted of a 3 x 3 in. NaJ(Tl) crystal with a 0.2 mm thick Be-window (HARSHAW INTEGRAL LINE) and a 200 channel analyser (LABEN).

By previous experiments, an excellent agreement was found between results determined by  $4\pi\beta$ -counting and  $4\pi\beta$ - $\gamma$ -coincidence measurements and analysis by means of the gamma crystal spectrometer, respectively, utilizing literature values (14) for the ratio of photopeak efficiency and total efficiency for the NaJ crystal used. This calibration of the crystal was executed with sources of Au-198, Nb-95, Cs-44 and Na-24. The deviation found between these two methods was about 1-2%.

The activation results obtained have been corrected for attenuation of the photopeak due to self-absorption in the detector foils and for coincidences.

The induced activity of Co-60 was determined in a relative method by gamma spectroscopy in comparing with a standard source of Co-60 having been calibrated with the  $4\pi\beta$ - $\gamma$ -coincidence method.

The thermal flux has been evaluated from the induced activity:

$$nv_0 = \frac{A_{\text{thermal}}}{\sigma_0}$$

applying the thermal cross-section  $\sigma_0$  instead of the effective cross-section  $\hat{\sigma}$  which includes also the epithermal and resonance production - a procedure being permitted because of the high share of thermal neutrons in our beam. A measuring error of  $\pm 5\%$  has to be expected. The thermal neutron flux of  $1.16 \times 10^{13}$  n/cm<sup>2</sup>sec evaluated at position 1.5 cm is somewhat smaller than the theoretical value for this point ( $2.5 \times 10^{13}$  n/cm<sup>2</sup>sec), probably due to absorption by the construction materials of the facility.

The epithermal neutron flux can be calculated from the induced activities of the cadmium covered Co and Au monitors. Assuming a  $1/E$  spectral distribution we write the activation integral for cadmium covered samples as:

$$A_{\text{Cd}} = \phi_0 \left( \int_{E_{\text{Cd}}}^{\infty} \frac{\sigma_r(E)}{E} dE + \int_{E_{\text{Cd}}}^{\infty} \frac{\sigma_{1/v}(E)}{E} dE \right)$$

where  $\phi_0$  is the flux per unit ln E interval,  $E_{\text{Cd}}$  ( $= 0.55$  eV) is the cadmium cut-off energy, and  $\sigma_r$  and  $\sigma_{1/v}$  are the resonance and  $1/v$  components of the total cross-section. The values used for the resonance integral of Au-197 and Co-59 are 1535 b and 71.9 b, respectively. The error of the flux evaluation is determined by the deviation of the real spectra from the assumed  $1/E$ -distribution (measuring error approx. 5%).

The fast neutron flux as indicated by the activation of the threshold detectors listed in Tab. 1 has been calculated following the method described in the papers of DI COLA and ROTA (5, 6). The values  $\sigma_i(E)$  utilized for evaluation have been determined by a critical discussion of recent literature data.

The mean reaction cross-section in a spectra  $\varphi(E)$  is defined as:

$$\bar{\sigma}_i = \frac{\int_0^{\infty} \sigma_i(E) \varphi(E) dE}{\int_0^{\infty} \varphi(E) dE}$$

The absolute values of the different reaction cross-sections  $\bar{\sigma}_i$  have been determined by normalization of  $\sigma$ -values calculated for a pure fission spectrum after CRANBERG (12) on  $\sigma$ -values evaluated from a real fission spectrum (converter).

At the positions 1, 31.5 and 52.5 cm (corresponding distances of 66, 96.5 and 117.5 cm from the core-center), the energy distribution of the fast neutrons has been calculated and is plotted in Fig. 16 together with a pure fission spectrum after CRANBERG (12), demonstrating good agreement between experimental curves and CRANBERG-spectrum at higher energies. Fig. 16 indicates also the influence of the weighting function  $W(E)$  to be applied in the analysis: curve a) at position 1 cm was obtained using a CRANBERG-spectrum, curve b) with a theoretically calculated spectrum (see ref. 10). There is noted a slight difference of the energy distribution but the influence on the integrated fast neutron flux is small ( $\pm 5\%$ )\*.

Fig. 16 shows further that the fast neutron spectrum does not vary remarkably with the distance. In three positions (1, 31.5 and 52.5 cm) the fast neutron flux was determined by integrating the spectrum obtained by application of 5 detectors (no. 5 - 10, Tab. 1) between the limits 0.75 and 1.25 MeV, respectively, and 7 MeV. The total error under consideration of measuring error, uncertainty of  $\sigma_i$ -values and analysis error is estimated to be in the latter case approx. 10%, in the former case (integration 0.75 - 7 MeV), the error approaches  $\pm 15\%$  due to the lower sensibility

---

\* In the spectra determined using the theoretically calculated as weighting function there are noticed deviations from the pure fission spectrum below 2 MeV and at 4 MeV which can be related - as shown in ref. 10 - to the relatively high removal cross-section of oxygen ( $D_2O$ ) and carbon (graphite) in these energy ranges.

of the monitors below 1.5 MeV. For other positions and core-configurations, the integrated fast neutron flux can be evaluated relatively in comparing the obtained induced activity of Ni-58 to the integrated flux in the three positions indicated above.

In Fig. 17 the integral neutron fluxes (thermal, epithermal and fast) are plotted as a function of distance. It is seen, that the flux spectrum is fairly well determined for all interesting positions in hole 4DH3 along 70 cm from the core-side end of the facility to the biological shielding, providing thus the execution of any irradiation experiment in this facility.

### 8. First results and experiences

The first experiment performed in the hole 4DH3 facility was a study of radiation enhanced ordering in Cu-Zn-alloys.

Point defects produced by neutrons enhance ordering processes in alpha-brass so that these will proceed also at temperatures at which ordering occurring as a result of thermally activated self-diffusion is negligible. The increase of degree of order is accompanied by a decrease of the electrical resistivity of the specimen. A typical resistivity curve of a Cu-36% Zn-sample under neutron irradiation (approx.  $2 \times 10^{11}$  n/cm<sup>2</sup>sec) is reproduced in Fig. 18.

From such curves the time for half completion has been taken as a measure of the amount of enhancement of the ordering process due to neutron irradiation.

A preliminary discussion of the results obtained was given at the March meeting of the American Physical Soc. in 1967 (9). A detailed discussion of the results is given in reference (10) and will be given elsewhere (11).

In conclusion we may state that the irradiation facility installed in hole 4DH3 of ISPRA-1 allows irradiations of suitable samples to be performed at different neutron fluxes and at temperatures between 30 and 900°C.

The resistance measuring equipment enables even unskilled people to execute irradiation experiments with high accuracy. Insertion and extraction of capsules is feasible without difficulties or danger for the operator.

The facility itself has now been in operation for almost two years without any troubles. Only the indication of the control thermocouples installed in-



side the facility (see par. 2.2) has changed slightly, probably due to radiation damage and/or transmutation in the thermo-electric material. But since for control purpose only relative temperature values are sufficient, this is of no importance.

### Acknowledgements

The authors respectfully acknowledge the collaboration with the staff of the Reactor Group of CCR Ispra under the leadership of Dr. QUEQUIN, who assisted in the installation of the facility and its operation.

We are particularly indebted to Drs. A. and M. BRESESTI of the Nuclear Chemistry Group of CCR Ispra for their valuable help in performing the neutron flux measurements.

The authors wish to thank M. PENKUHN - Theory Calculation Reactor Group of CCR Ispra - for his contribution to the calculations of the radiation shielding of the facility.

Finally we appreciate gratefully the participation of Dr. SPINDLER in a number of the irradiation experiments.

9. References

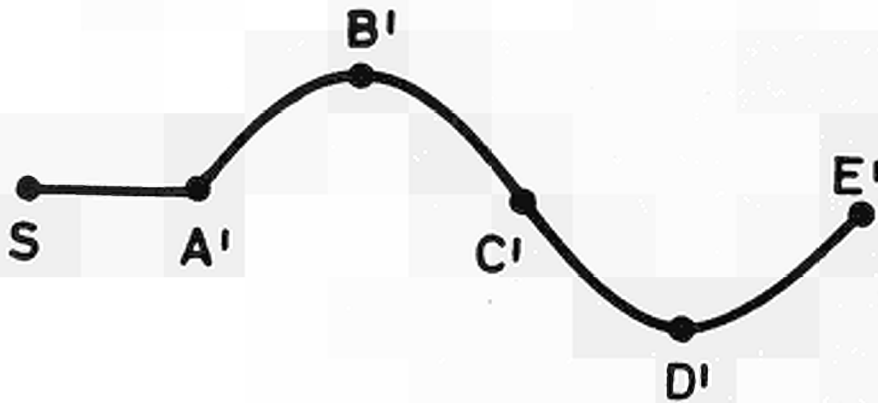
- (1) R. GEISER, HFR Information Meeting Petten, Dec. 7-8, (1967), p 51
- (2) C. BASSANI, "A Liquid Nitrogen Facility for Radiation Damage Studies in the 4GV1 Beam of ISPRA-1 Reactor", to be published
- (3) C. BASSANI and P. CERUTTI, "Gamma Heat Generation in the 4GV1 Beam of the ISPRA-1 Reactor", EUR-2178.e, (1964)
- (4) R.R. COLTMANN, C.E. KLABUNDE, D.L. McDONALD and J.K. REDMAN, J. Appl. Phys., 33, 3509 (1962); see also: R.R. COLTMANN, C.E. KLABUNDE, and J.K. REDMAN, Phys. Rev., 156, 715 (1967)
- (5) G. DI COLA and A. ROTA, "RDMN - A Code for Fast Neutron Spectra Determination by Activation Analysis", EUR-2985.e (1966)
- (6) G. DI COLA and A. ROTA, Nucl. Sci. and Eng., 23, 344 (1965)
- (7) A.M. BRESESTI, M. BRESESTI and R.A. RYDIN, Nucl. Sci and Eng. (1967)
- (8) M. BRESESTI, private communication 1967
- (9) W. SCHÜLE and E. LANG, "Enhancement of Diffusion During Reactor Irradiation", Bull. Am. Phys. Soc. II, 12, 3, 325 (1967)
- (10) E. LANG, "Über die Wanderung von atomaren Fehlstellen in - Messing während Neutronenbestrahlung und nach Abschrecken", Thesis, Techn. Hochschule Braunschweig, 1967
- (11) W. SCHÜLE and E. LANG, "Radiation Enhanced Ordering Processes in  $\alpha$ -brass", to be published
- (12) L. CRANBERG, Phys. Rev., 43, 662 (1956)
- (13) H. GOLDSTEIN, "Fundamental Aspects of Radiation Shielding", Adison-Wesley 1959, p 18 ff.
- (14) L. HEATH, "Scintillation Spectrometry Gamma Ray Spectrum Catalogue, IDO - 16 880 - 1 Philips Petroleum Company (1964)

## 10. APPENDIX - Calculation of the radiation shielding for the irradiation facility

### 10.1. Shielding efficiency of a tube in spiral form

We assume as follows:

The neutron flux in the MeV-range at the core end of the sample tube is (with a safety factor 2)  $5 \times 10^{11}$  n/cm<sup>2</sup>sec; the diameter of the tube is 5.3 cm. The axis of the tube has the form of a spiral passing through the 1.30 m thick shielding plug in one complete turn. The axis may be considered as a deformed sine curve ABCDE, the middle part of which is laterally shifted out of the plane ADE, so that with little changed profile, (left in the sketch) the point C'' in the ground plane (right) falls beside the axis A''B''D''E''.



The radiation intensity at the exit of the tube is composed of two contributions: first the number of neutrons directly scattered through the tube to the outside, and second the contribution of the neutrons passing through the shielding materials, thereby being scattered and slowed down.

#### 10.1.1. Neutrons directly scattered through the tube

The neutron source has a diameter of 10 cm (diameter of the beam hole) corresponding to a surface of approx. 80 cm<sup>2</sup>. The radiation is isotropically directed into the outside hemisphere; thus we have at the beginning of the wound part of the tube, i. e. at point A, 80 cm from the core-end, a neutron intensity of

$$I_A = \frac{2\phi F_1 \times F_0}{4 r_1^2 \cdot \pi} \quad (1)$$

where:  $\phi$  = neutron flux =  $5 \times 10^{11}$  n/cm<sup>2</sup> sec  
 $F_0$  = surface of the neutron source = 80 cm<sup>2</sup>  
 $F_1$  = cross-section of the sample tube = 22 cm<sup>2</sup>  
 $r_1$  = distance point A (of the tube) to source S = 80 cm

A factor 2 safety factor stems from the assumption that the total radiation is isotropically directed into the reactor wall-side hemisphere. Equation (1) yields

$$I_A = 0.22 \times 10^{11} \text{ n/sec}$$

If a neutron is scattered by a volume, the integration over this volume yields in case that the angle of incidence is equal to the reflection angle, a scattered intensity which is half the value for equivalent point scattering. Since hydrogen scatters in the forward direction twice as strong as other materials do, and since the shielding of the irradiation facility (see Fig. 3) is about half hydrogen-containing material (polyethylene, density 0.95 g/cm<sup>3</sup>) we have to introduce a correction factor  $k = 1/2 \times 2 + 1/2 \times 1 = 3/2$ , thereby taking into account the more efficient scattering power of hydrogen. The scattered neutron intensity at point B of our spiral line (see sketch) is given by:

$$I_B = I_A \frac{s k F_1}{4 \pi r_2^2} = 0.22 \times 10^{11} \times 1.24 \times 10^{-3} \quad (2)$$

where  $I_A$  = intensity at point A =  $0.22 \times 10^{11}$  n/sec  
 $k$  = correction for hydrogen-containing material = 3/2  
 $s$  = factor for taking into account volume scattering (instead of point scattering) = 1/2  
 $r_2$  = distance A - B = 32.5 cm

Since the sections B-C, C-D, D-E similarly reduce the scattered radiation by the factor  $1.24 \times 10^{-3}$  we obtain for the intensity at the sample exit E:

$$I_E = 0.22 \times 10^{11} \times (1.24 \times 10^{-3})^4 = 5 \times 10^{-2} \text{ n/sec} \quad (3)$$

With the sample tube's cross-section of  $22 \text{ cm}^2$  this intensity corresponds to a neutron flux of  $2.5 \times 10^{-3}$  yielding a fast neutron dose rate of  $3.8 \times 10^{-4}$  mrem/h. Even taking into account the thermal and epithermal neutron contribution, each of which may be 1 1/2 times the fast neutron flux, we get for the total dose rate due to neutrons scattered directly through the tube at maximum  $2 \times 10^{-3}$  mrem/h. Thus the radiation contributed by neutrons scattered along the sample tube may be neglected.

### 10.1.2. Neutrons penetrating the shielding materials

By locating the sample tube within the shielding plug in form of a spiral line, the mean free path length of a neutron in air will not exceed 30 cm. The remaining shielding thickness amounts to  $130 - 30 = 100$  cm. It will further be supposed that this shielding consists of a 10 cm thick lead layer, followed by a layer of reinforced concrete (density  $4.5 \text{ g/cm}^3$ ) of 45 cm thickness and a 45 cm thick layer of polyethylene<sup>+</sup>. For shielding purposes it is of minor importance whether this mixture is homogeneous or whether it is made up of plates of some centimeter thickness. Since the shielding consists by half of hydrogen-containing material (polyethylene  $(\text{CH}_2)_n$ ), the ALBERT-WELTON-formula is used for the calculation of the neutron flux at the sample tube exit.

$$\phi_f = \frac{2.9 Q}{4\pi r^2} e^{-\sum u_i x_i} \cdot r_{\text{H}_2\text{O}}^{0.29} \cdot e^{-0.928 (r_{\text{H}_2\text{O}})^{0.58}} \quad (4)$$

where:  $\phi_f$  = fast neutron flux

$Q$  = source intensity

$r$  = distance source-detector

$u_i$  = macroscopic removal-cross-section of material  $i$

$x_i$  = layer thickness of material  $i$

$r_{\text{H}_2\text{O}}$  = equivalent water thickness of hydrogen-containing material

Taking into consideration only those neutrons arriving at the tube exit E which have passed through the entrance A from a point E at the tube exit only  $58 \text{ cm}^2$  of the  $80 \text{ cm}^2$  large neutron source are visible, according to:

<sup>+</sup>) In reality the shielding efficiency has been improved by including a 3.5 cm thick layer of Boral.

$$F_E = \frac{F_1 \times l_0^2}{l_1^2} \quad (5)$$

where:  $F_1$  = cross-section of the sample tube  
 $l_0$  = distance hole top S - tube exit E  
 $l_1$  = distance A-E

With a neutron flux of  $5 \times 10^{11}$  n/cm<sup>2</sup>sec we obtain a source intensity of  $Q = 2.90 \times 10^{13}$  n/sec.

The macroscopic removal-cross-section  $\mu_i$  is evaluated by the following formula:

$$\mu_i = L/A \times g_i \times \sigma_i \quad (6)$$

where:  $L$  = Loschmidt's number  
 $A$  = atomic weight  
 $g_i$  = specific weight (density)  
 $\sigma_i$  = atomic removal-cross-section (in barn)

For the concrete used in the shielding, we assume a ferrophosphorous-concrete of density 4.5 g/cm<sup>3</sup> as described in ANL-5800.

Since at the temperatures of more than 100°C existing in the facility, the water contained in the concrete is evaporated, we extrapolate its properties to the water content zero, its removal-cross-section being then  $\mu_B = 0.105$  cm<sup>-1</sup>. The carbon in the polyethylene ( $g = 0.95$  g/cm<sup>3</sup>) has the specific weight:

$$g_C = \frac{\rho(\text{CH}_2)_n \cdot A_C}{A(\text{CH}_2)_n} = \frac{0.95 \times 12}{14} = 0.81 \text{ g/cm}^3$$

With an atomic removal-cross-section of 0.81 barn, for the macroscopic removal-cross-section follows according to formula (6) that  $\mu_C = 0.033$  cm<sup>-1</sup>. Correspondingly, the density of hydrogen in polyethylene amounts to 0.136 g/cm<sup>3</sup>, i. e. the density of hydrogen in  $(\text{CH}_2)_n$  is 1.22 times higher than in water. Hence, 45 cm  $(\text{CH}_2)_n$  correspond to 55 cm water, as concerns the contents of hydrogen i. e. shielding efficiency.

For the macroscopic removal-cross-section of lead ( $A = 207$ ,  $g = 11.3$  g/cm<sup>3</sup>),  $\sigma = 3.53$  barn) we obtain:  $\mu_{Pb} = 0.116$  cm<sup>-1</sup>.

The distance between source and detector corresponds to the total length of the facility  $l_0 = 2.10$  m.

Furthermore, the neutron radiation is assumed to be scattered isotropically into the outside (reactor wall-side) hemisphere, thus yielding a safety factor of 2.

Then we have to write the ALBERT-WELTON-formula in the following way:

$$\phi_f = \frac{2.2 \cdot \phi}{2 \pi r^2} \exp \left\{ -\mu_c \cdot x_c - \mu_B \cdot x_B - \mu_{Pb} \cdot x_{Pb} \right\} \cdot (r_{H_2O})^{0.29} \exp \left\{ -0.928 (r_{H_2O})^{0.58} \right\} \quad (7)$$

Inserting the values given in the foregoing, the calculation yields:

$$\phi_f = 42.8 \text{ n/cm}^2 \text{ sec.}$$

This last neutron flux gives a dose rate of  $D_f = 6.5$  mrem/h.

### 10.2. Additional shielding and total dose rate

An additional shielding can be achieved by filling the junction box of the beam hole 4DH3 (see Figs. 2, 3) with an additional 20 cm layer of polyethylene and a 10 cm thick wall of lead bricklets.

The lead layer does not significantly attenuate the fast neutrons, therefore it will not be taken into consideration. (According to the removal-theory it would add an attenuation factor of 3, providing thus additional safety). The external lead layer serves mainly as shielding against gamma radiation produced by thermal neutron capture.

For the 20 cm polyethylene layer, the calculation yields a reduction of the fast dose rate  $D_f$  by a factor 10, i. e. in front of the beam hole there should not arise a fast neutron dose rate higher than 0.7 mrem/h.

The thermal and epithermal dose can be neglected in comparison to the fast dose rate  $D_f$ . In an infinitely extended medium, both would be  $1 \frac{1}{2}$  times the fast flux,  $D_f$  (together  $3 D_f$ ). However, the thermal and epithermal neutrons are distributed over an area of the magnitude of  $\pi(\sqrt{2 \tau_{th}})^2$ , where  $\tau_{th}$  = Fermi age of thermal neutrons, in polyethylene amounting to approx.  $30 \text{ cm}^2$ . That means we should have to calculate for the thermal

neutrons with a cross-section of the tube of approx.  $190 \text{ cm}^2$  instead of  $22 \text{ cm}^2$  as done above. Thereby follows a reduction of the thermal neutron flux by a factor  $190/22 = 8.5$ .

Furthermore, this neutron flux does not exist at the exit E of the sample tube but at average  $1/2 \times 30 \text{ cm}$  more inside. Assuming a cosinus-shaped tube, at E arrives only the part:

$$\frac{22}{\pi \cdot 15^2} = 1/32$$

That means in total a reduction by a factor  $8.5 \times 32 = 270$ . Even with a safety factor 3, the contribution of the thermal and epithermal neutrons to the dose rate amounts only to:

$$\frac{3 \times 3 \times 7}{270} \approx 0.23 \text{ mrem/h}$$

The total dose rate including slow neutrons therefore should not exceed 1 mrem/h - as we found it in reality (see par. 2.2).

Finally, we may answer the following questions:

- 1) How does the dose rate depend on the neutron flux of the source (reactor power) level? - According to the ALBERT-WELTON-formula, the dose rate is directly proportional to the neutron flux.
- 2) How does the dose rate depend on the cross-section of the tube? - The portion of neutrons reflected directly through the sample tube is, because it is scattered 4 times, proportional to the fourth power of the cross-section. The portion passing through the shielding materials, this being by far the major contribution, is proportional to the first power of cross-section.
- 3) What additional safety factors might perhaps be added? - Lack of precise knowledge of the source intensity approximations in the geometry and in the effective removal-cross-sections might give rise to maximum error of a factor of 5.
- 4) May any other radiation than the neutron radiation, considered above, give a noticeable contribution to the total dose rate? - High energy protons are produced by slow neutron capture in the iron of the shielding concrete. But this is adequately suppressed by the



external 10 cm thick layer of lead.

### 10.3. Radiation resistance of polyethylene

Behind the 10 cm lead and the 60 cm thick layer of concrete (of which we subtract 15 cm for taking into account the empty sample tube), there exists a fast neutron flux of:

$$\phi_f = \frac{F_o \cdot \phi_o}{2\pi l_1^2} \cdot \exp \left\{ -\mu_B \cdot x_B - \mu_{Pb} \cdot x_{Pb} \right\} \quad (8)$$

where:

$$F_o = 80 \text{ cm}^2$$

$$Q = 5 \times 10^{11} \text{ n/cm}^2 \text{ sec}$$

$$l_1 = 80 + 10 + 45 = 135 \text{ cm}$$

$$\mu_B = 0.105 \text{ cm}^{-1}$$

$$x_B = 45 \text{ cm}$$

$$\mu_{Pb} = 0.116 \text{ cm}^{-1}$$

$$x_{Pb} = 10 \text{ cm}$$

These values inserted, we obtain  $\phi_f = 1 \times 10^6 \text{ n/cm}^2 \text{ sec}$ .

In tissue (of the composition  $C_7H_{70}O_{32}N_2$ ) this neutron flux produces approx. 70 rad/h (see ref. 13), hereby assumed that 1 gr  $(CH_2)_n$  and 1 gr tissue absorb comparably. To reach the maximum permissible limit of radiation resistance of  $10^8$  rad, an irradiation of  $1.4 \times 10^6$  h or 160 years would be needed.

It may be interesting to know how much heat is developed by the absorption process: Since 1 rad is equivalent to 100 erg/gr, we have a specific heat production of 7000 erg/gr. That corresponds to a specific dose rate of about  $2 \text{ erg/gr} = 0.2 \mu\text{W/gr}$  and this value will also be achieved only at the first few centimeters of the polyethylene layer.

## 11. List of Figure Captions

- Fig. 1 Irradiation devices: a) Loop, b) Capsule, according to GEISER (1)
- Fig. 2 Sectional view of reactor ISPRA-1 with showing the position of the experimental holes
- Fig. 3 Sectional view of the irradiation facility in beam hole 4DH3 of ISPRA-1 (not to scale)
- Fig. 4 Detail of the bayonet flange used for quick closing of the sample tube
- Fig. 5 Schematic circuit diagram of the safety installations for the vacuum systems of the irradiation facility
- Fig. 6 Schematic diagram of the safety installations for the sample heating
- Fig. 7 View of the control and auxiliary equipment for the irradiation facility in hole 4DH3
- 1) Rack with measuring and control instruments for the vacuum systems,
  - 2) Rack with cooling water control instruments, partly hidden,
  - 3) Vacuum cleaner acting at the sample tube exit for capsule introduction and extraction operation,
  - 4) High vacuum equipment for vacuum jacket,
  - 5) High vacuum equipment for sample tube,
  - 6) Connector pannel,
  - 7) Bayonet flange of the sample tube,
  - 8) Filter system,
  - 9) Gamma-radiation-monitor, connected to filter system.
- Fig. 8 Sample capsules with heater for irradiation of non-fissile material to temperatures of  $400^{\circ}\text{C}$
- Fig. 9 View of a sample completely mounted on its sampleholder
- Fig. 10 Design of a capsule for irradiations of fissile material and/or irradiation experiments at higher temperatures (max.  $900^{\circ}\text{C}$ )
- Fig. 11 Schematic diagram of the extraction facility
- Fig. 12 View of the extraction facility and transfer vessel in operation at the reactor.
- Fig. 13 Schematic wiring diagram of the measuring circuit and the automatic DC constant current controller.
- Fig. 14 View of the measuring and control equipment at the surveyor's place (at a preliminary state of installation):
- 1) DC constant current controller,
  - 2) TINSLEY-Galvanometer with amplifier,
  - 3) Potentiometer for measuring potential drop,

- 4) Bridge for temperature measurements,
- 5) Stabilized power supply for heater current,
- 6) Rack including temperature controller for sample heating, 12-point-recorder for temperatures of the facility, temperature control instruments for cooling water circuit.

Fig. 15 Energy Spectra of the reaction and thermal capture cross-sections of the detectors used for neutron flux measurements

Fig. 16 Fast neutron energy distribution at 3 positions in hole 4DH3 of ISPRA-1. Curves a) and b), respectively, have been evaluated by using different weighting functions, see ref (9). For comparison also a pure fission spectrum according to CRANBERG (11) is plotted

Fig. 17 Integrated neutron flux (thermal, epithermal and fast) in hole 4DH3 at 5 MW reactor power as a function of distance from core-side end of the irradiation facility.

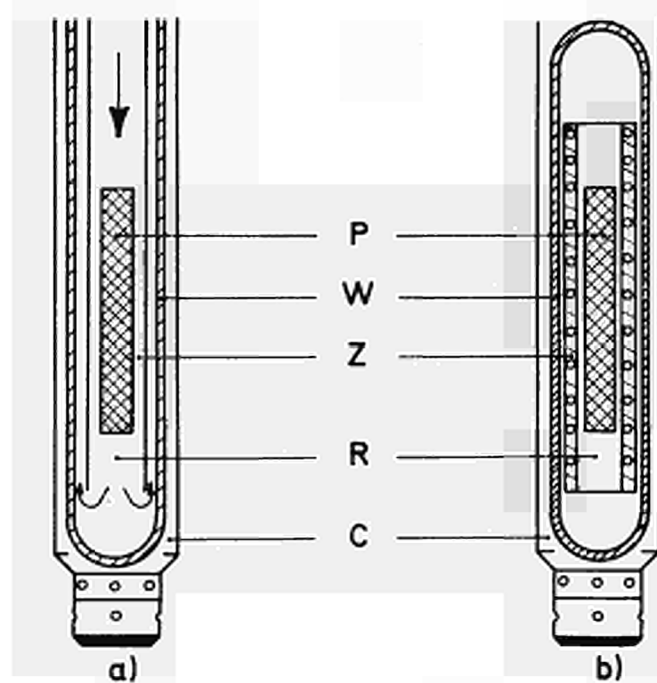
Fig. 18 Typical resistivity-time curve of an  $\alpha$ -brass sample under neutron irradiation. Plotted vertically is the resistivity increment  $\Delta \rho / \rho_0 (\%)$ ; this makes it unnecessary to determine the geometrical dimensions of the sample

Table 1: Detector elements and dosimetry parameters for neutron flux measurements, data according to ref (8)

TABLE 1 - DETECTOR ELEMENTS AND DOSIMETRY PARAMETERS FOR NEUTRON  
FLUX MEASUREMENTS, data according to (8)

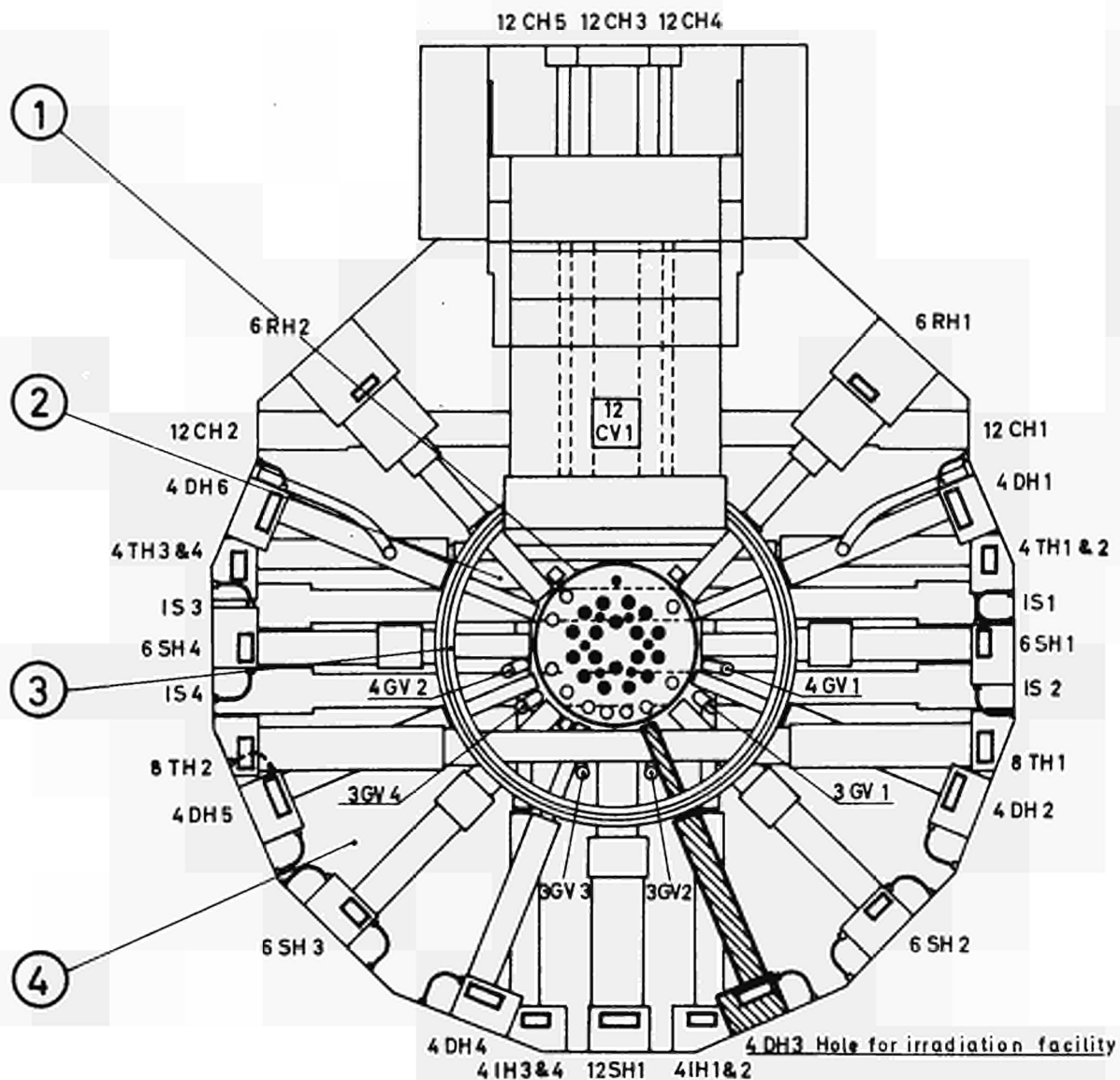
Detector- element	Nuclear Reaction	Cd- shielding	Threshold energy	Sensibility max.	Mean reaction cross-section	Half-live- time of mea- sured nuclide	Measured $\gamma$ -Intensity $\gamma$ -energy MeV	
1. Co	$\text{Co}^{59}(n,\gamma)\text{Co}^{60}$	no	-	-	37.4 b	5.27 a	1.17/1.33	100/100
2. Au	$\text{Au}^{197}(n,\gamma)\text{Au}^{198}$	no	-	-	98.8 b	2.69 a	0.411	96
3. Au	$\text{Au}^{197}(n,\gamma)\text{Au}^{198}$	yes	$E_{\text{Cd}}=0.55 \text{ eV}$	4.9 eV	1535 b	2.69 a	0.411	96
4. Co	$\text{Co}^{59}(n,\gamma)\text{Co}^{60}$	yes	$E_{\text{Cd}}=0.55 \text{ eV}$	132.0 eV	71.9 b	5.27 a	1.17/1.33	100/100
5. In	$\text{In}^{115}(n,n')\text{In}^{115\text{m}}$	yes	0.5 MeV	2.2 MeV	180 mb	4.5 h	0.335	46
6. Ni	$\text{Ni}^{58}(n,p)\text{Co}^{58}$	yes	1.5 MeV	3.5 MeV	106 mb	71.3 d	0.810+0.860	101
7. Fe	$\text{Fe}^{56}(n,p)\text{Mn}^{56}$	yes	4.5 MeV	7.3 MeV	1.08 mb	2.58 h	0.845	99
8. Mg	$\text{Mg}^{24}(n,p)\text{Na}^{24}$	yes	5.5 MeV	7.5 MeV	1.46 mb	15.0 h	1.368	100
9. Al	$\text{Al}^{27}(n,\alpha)\text{Na}^{24}$	yes	5.8 MeV	8.0 MeV	0.71 mb	15.0 h	1.368	100
10. Fe	$\text{Fe}^{54}(n,p)\text{Mn}^{54}$	yes	2.0 MeV	4.0 MeV	65.4 mb	303 d	0.835	100

FIGURE 1



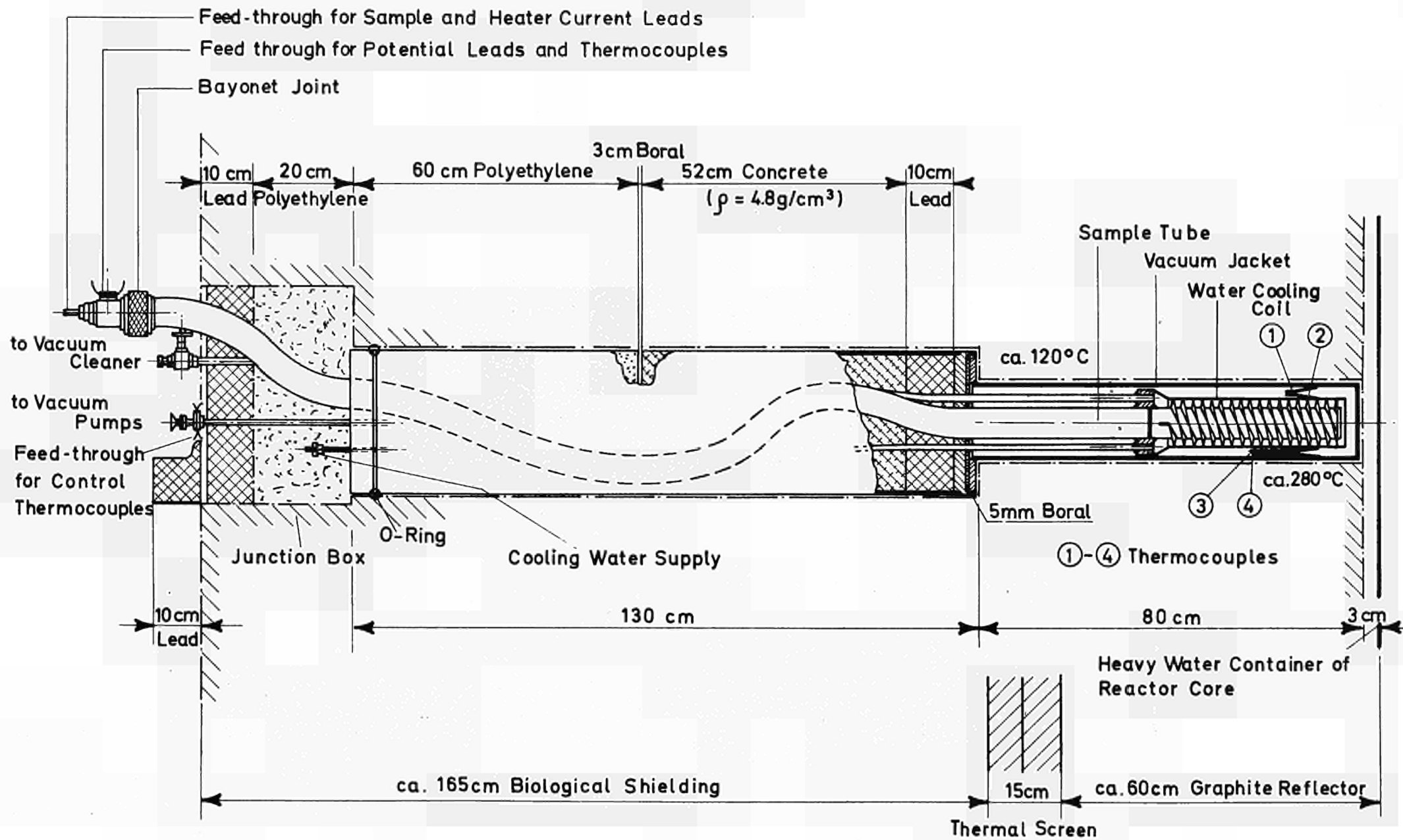
P Material Sample  
W Wall  
Z Thermal Barrier  
R Irradiation Room  
C Reactor Hole

FIGURE 2



- ① Heavy water container with reactor core
- ② Graphite reflector
- ③ Thermal shielding
- ④ Biological shielding made of reinforced concrete
- Fuel element
- Control rod
- Regulation rod
- Free fuel position, partly occupied by irradiation rigs

FIGURE 3



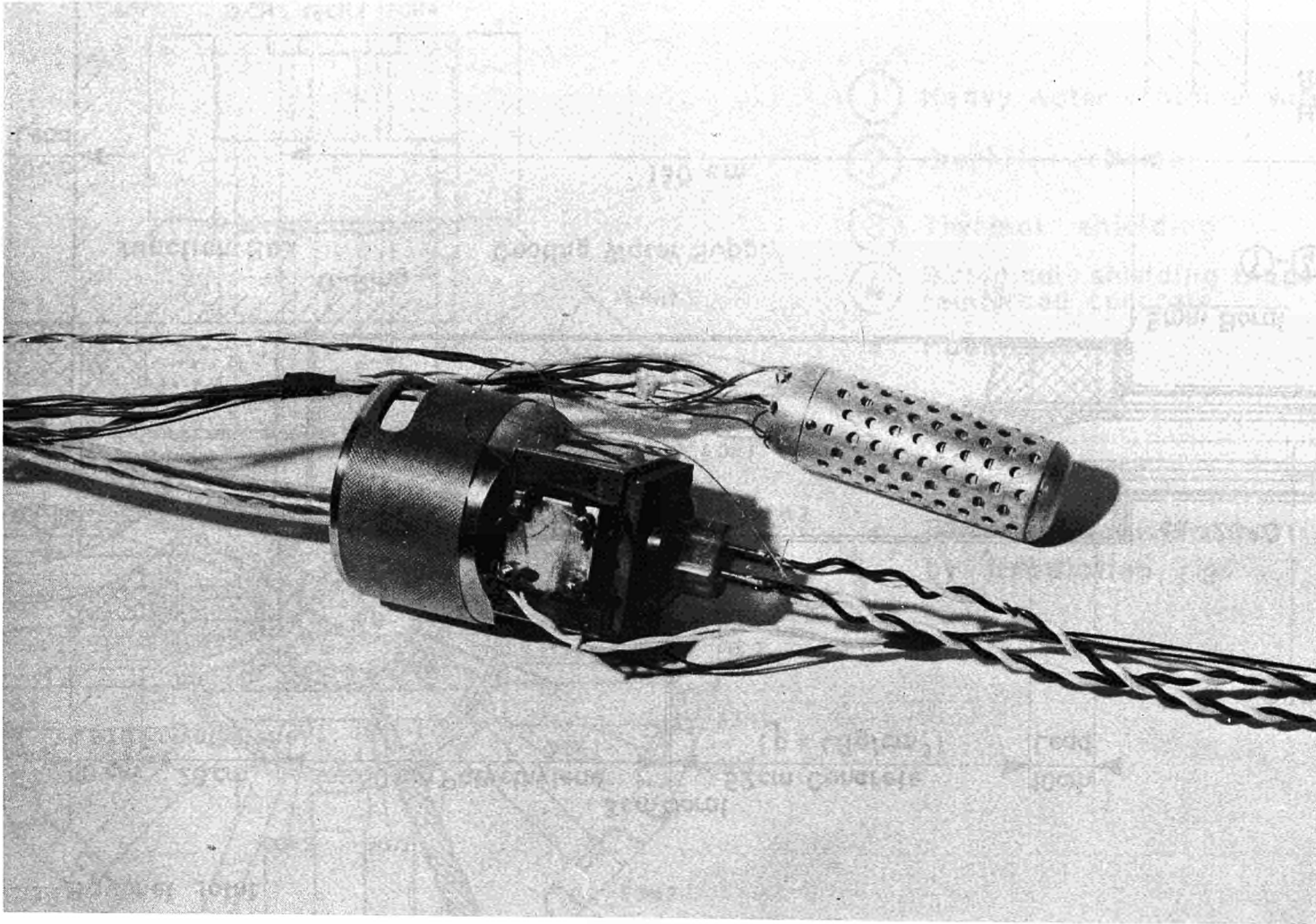


Fig. 4



FIGURE 5

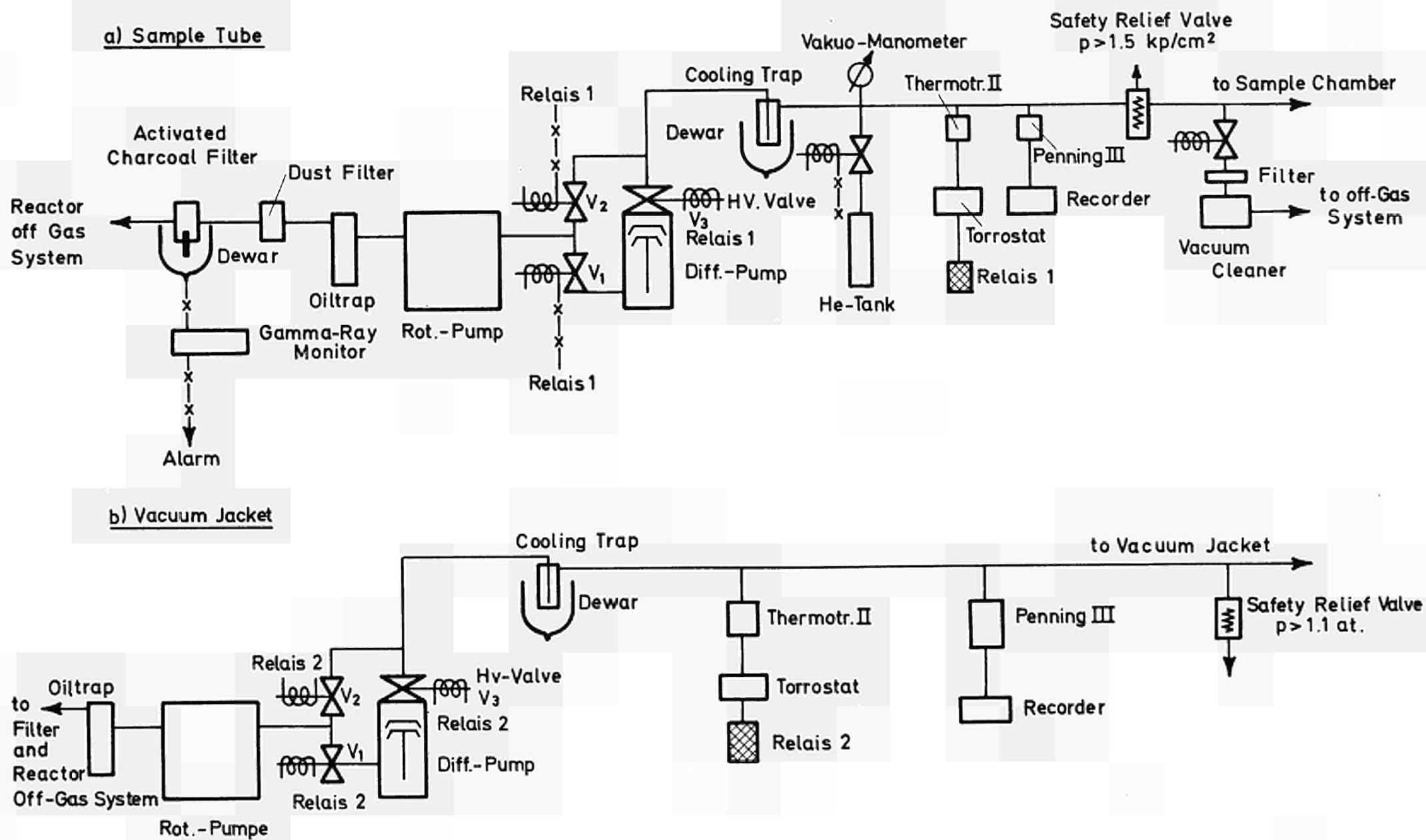
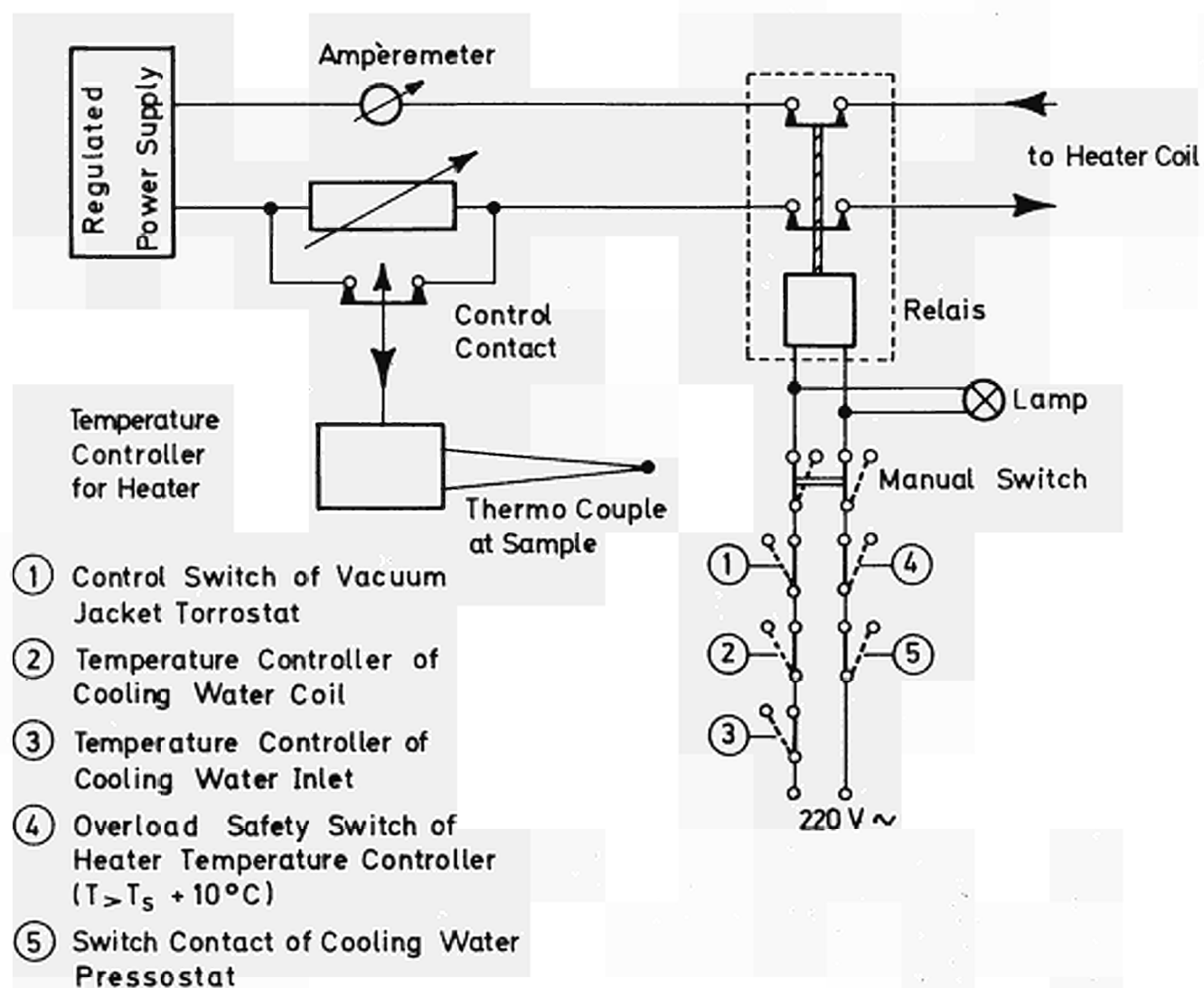


FIGURE 6



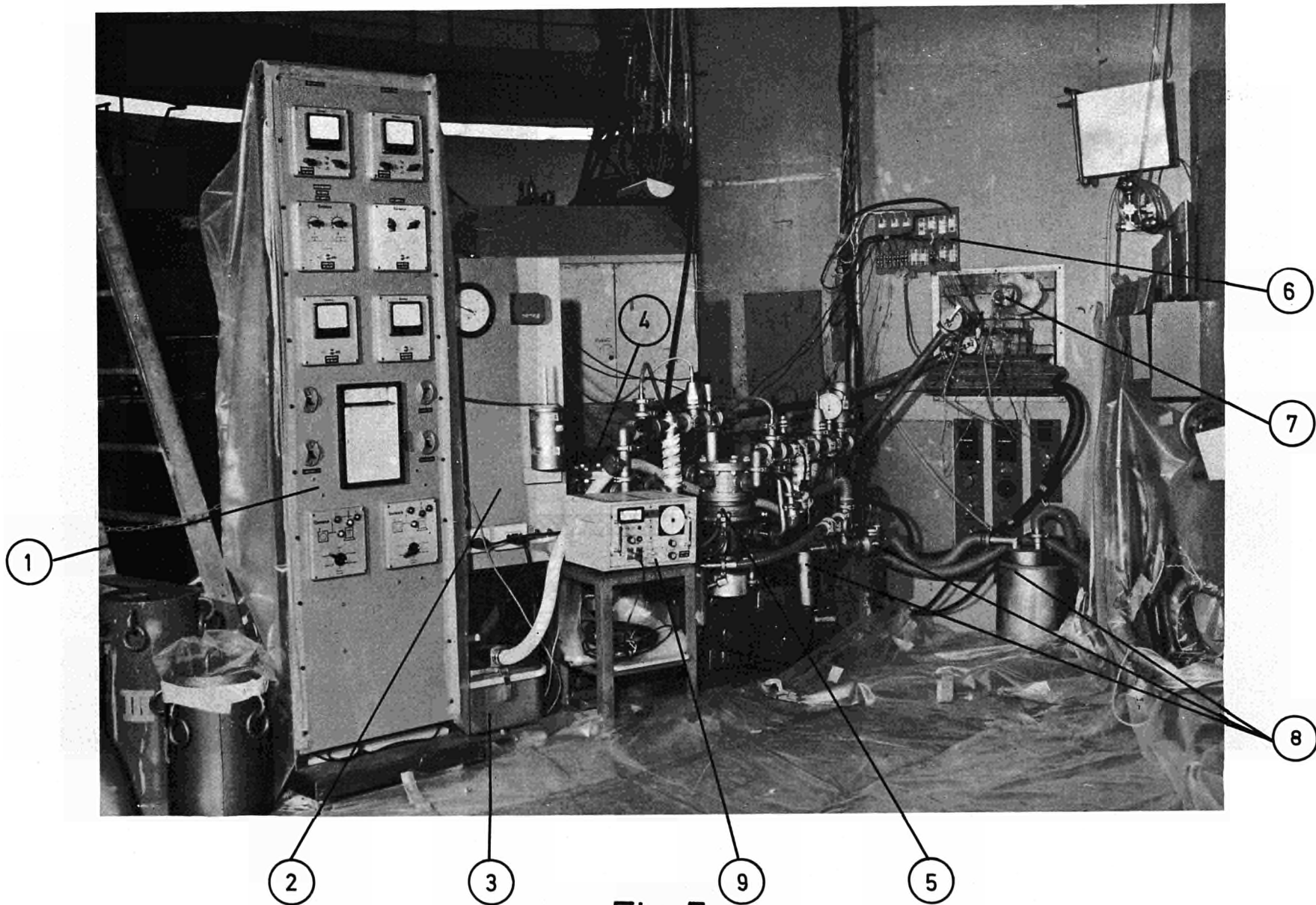


Fig 7

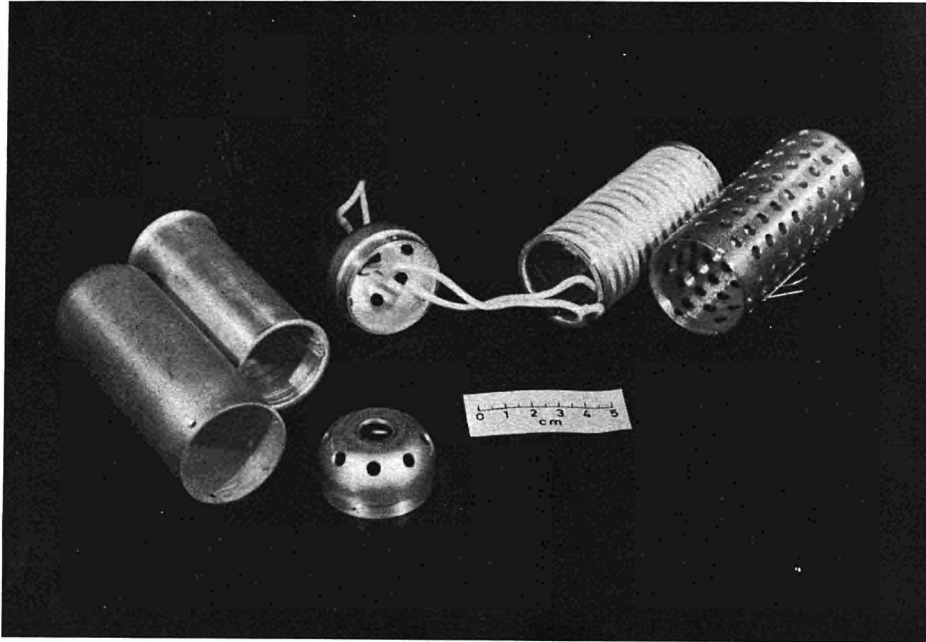


Fig. 8

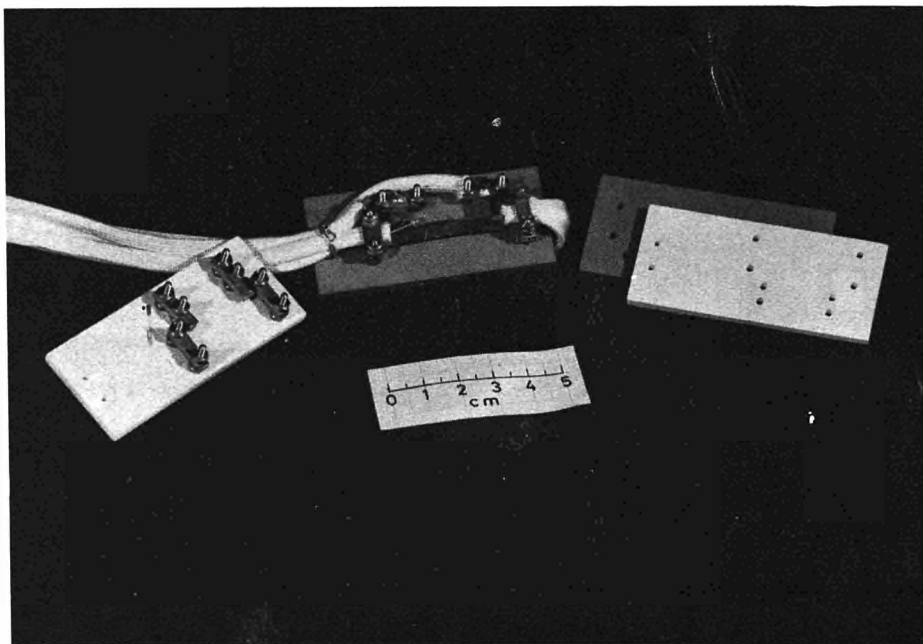


Fig. 9

FIGURE 10

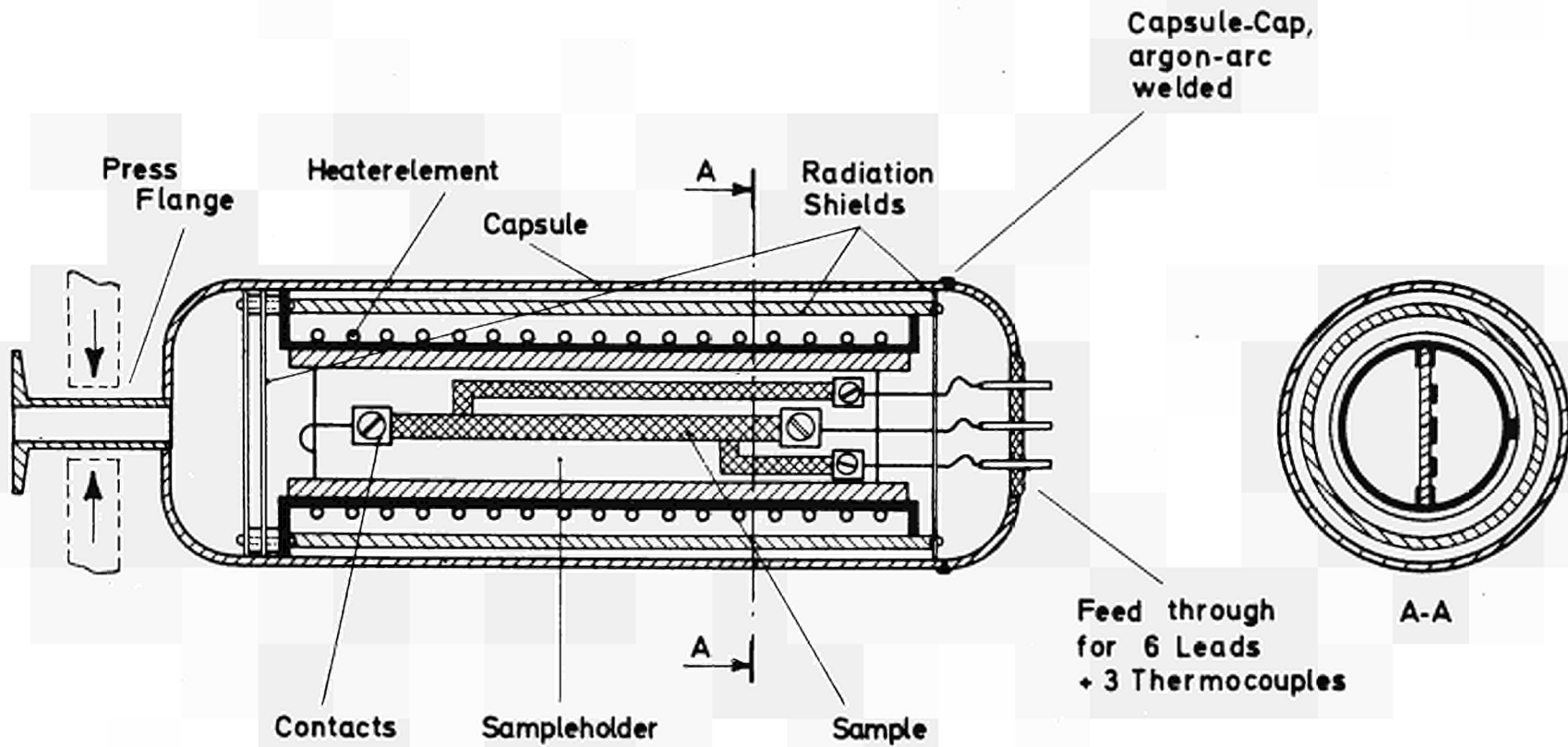


FIGURE 11

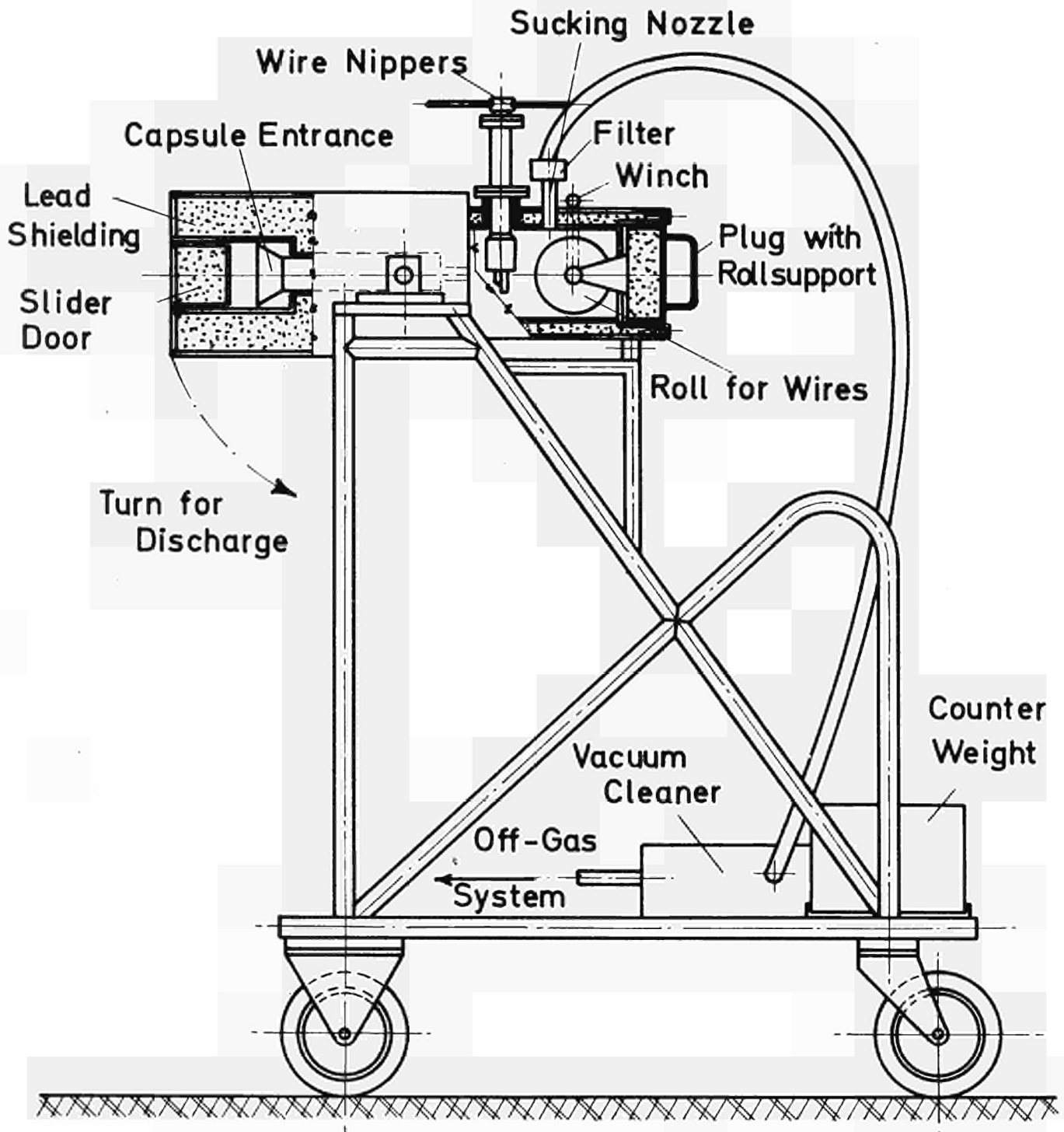




Fig. 12

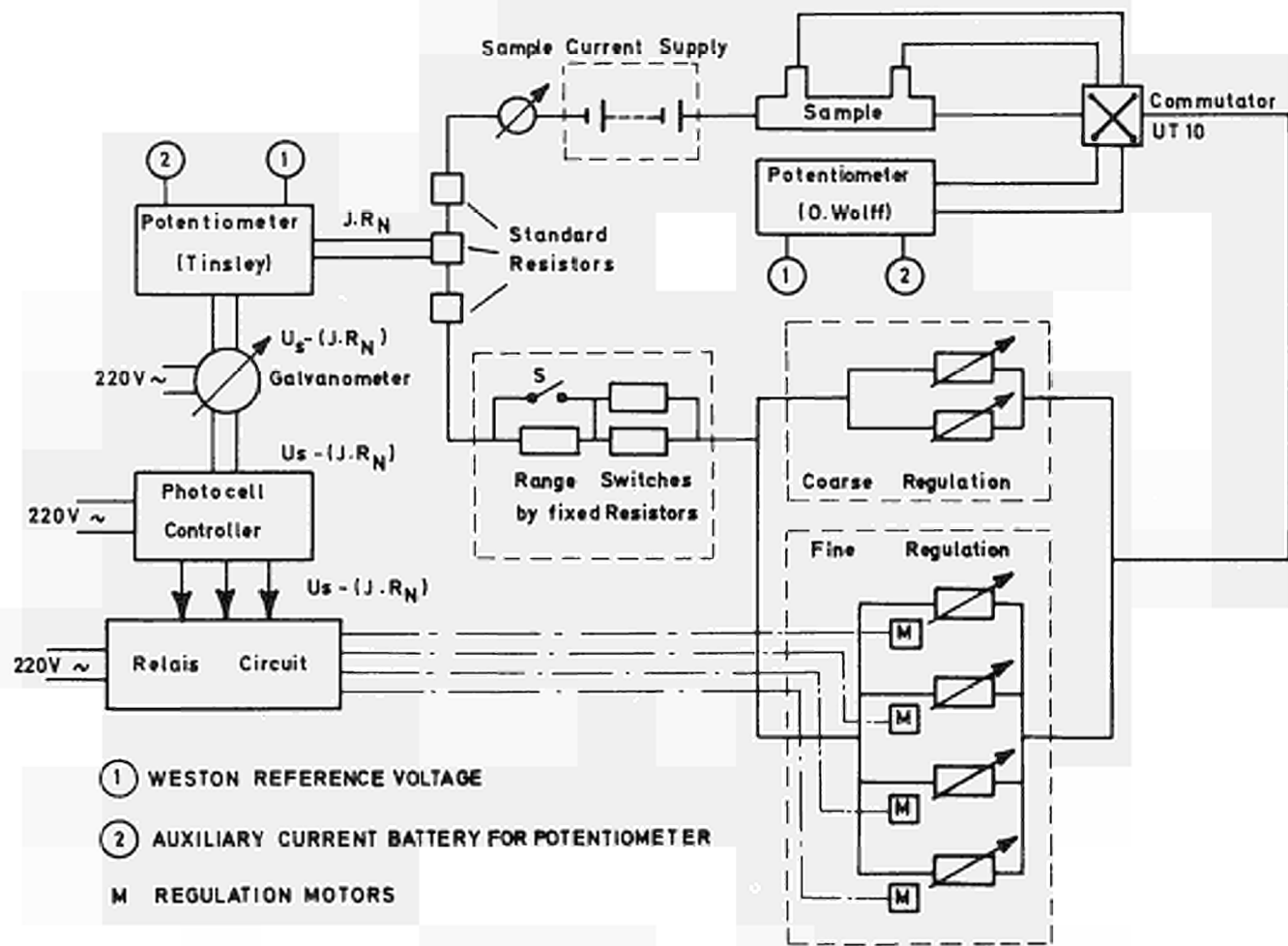


FIGURE 13



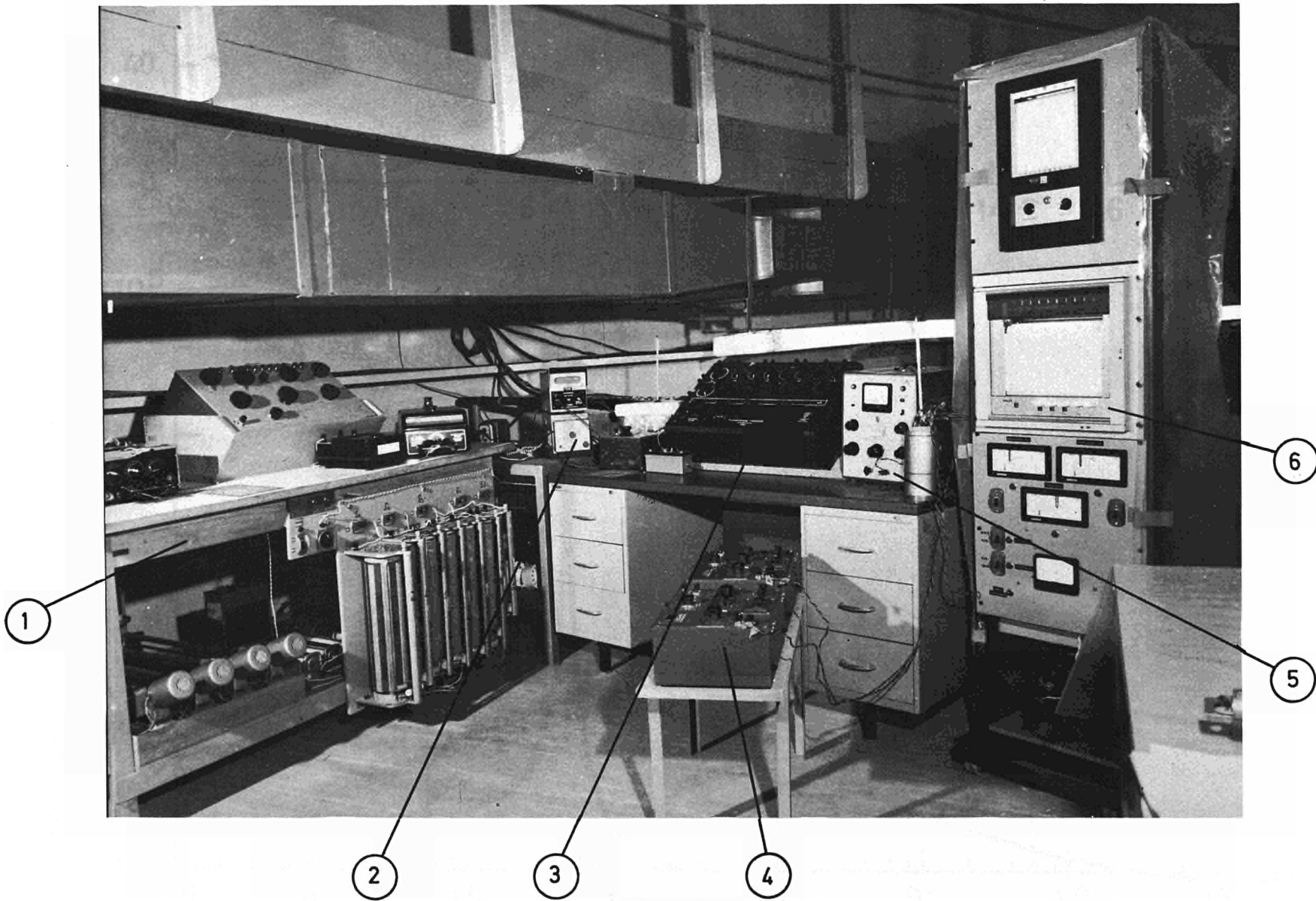


Fig. 14



FIGURE 15

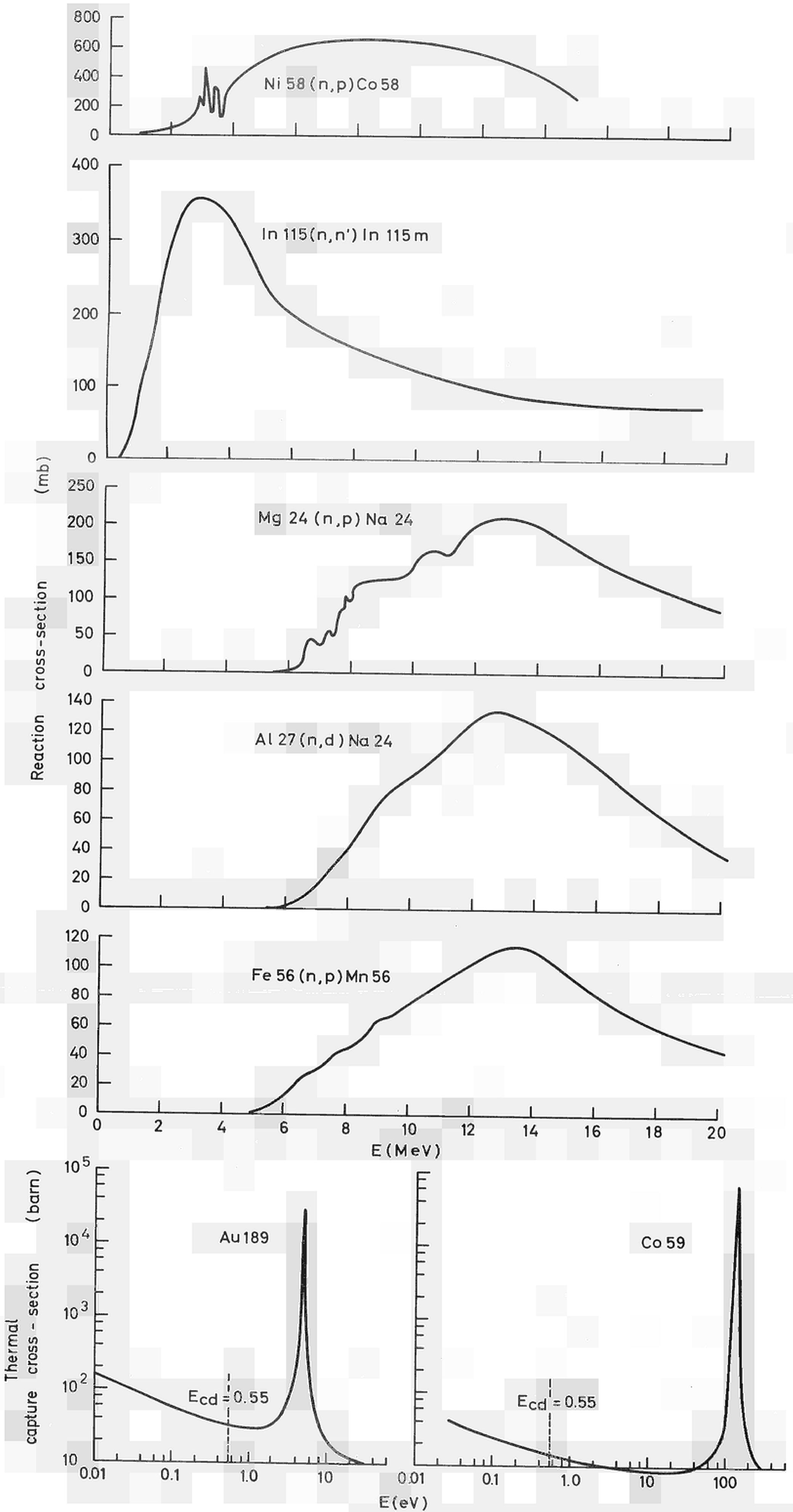
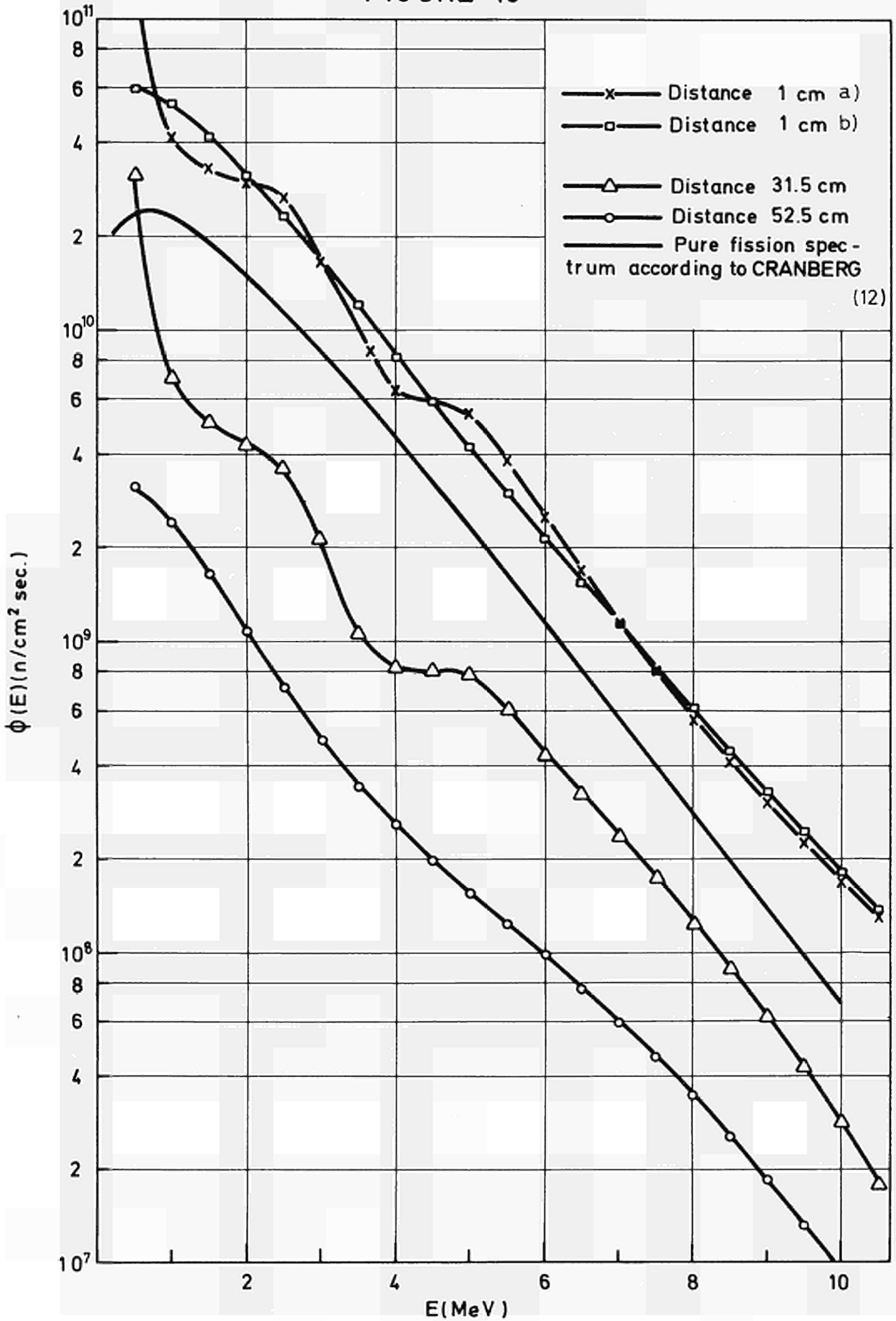




FIGURE 16



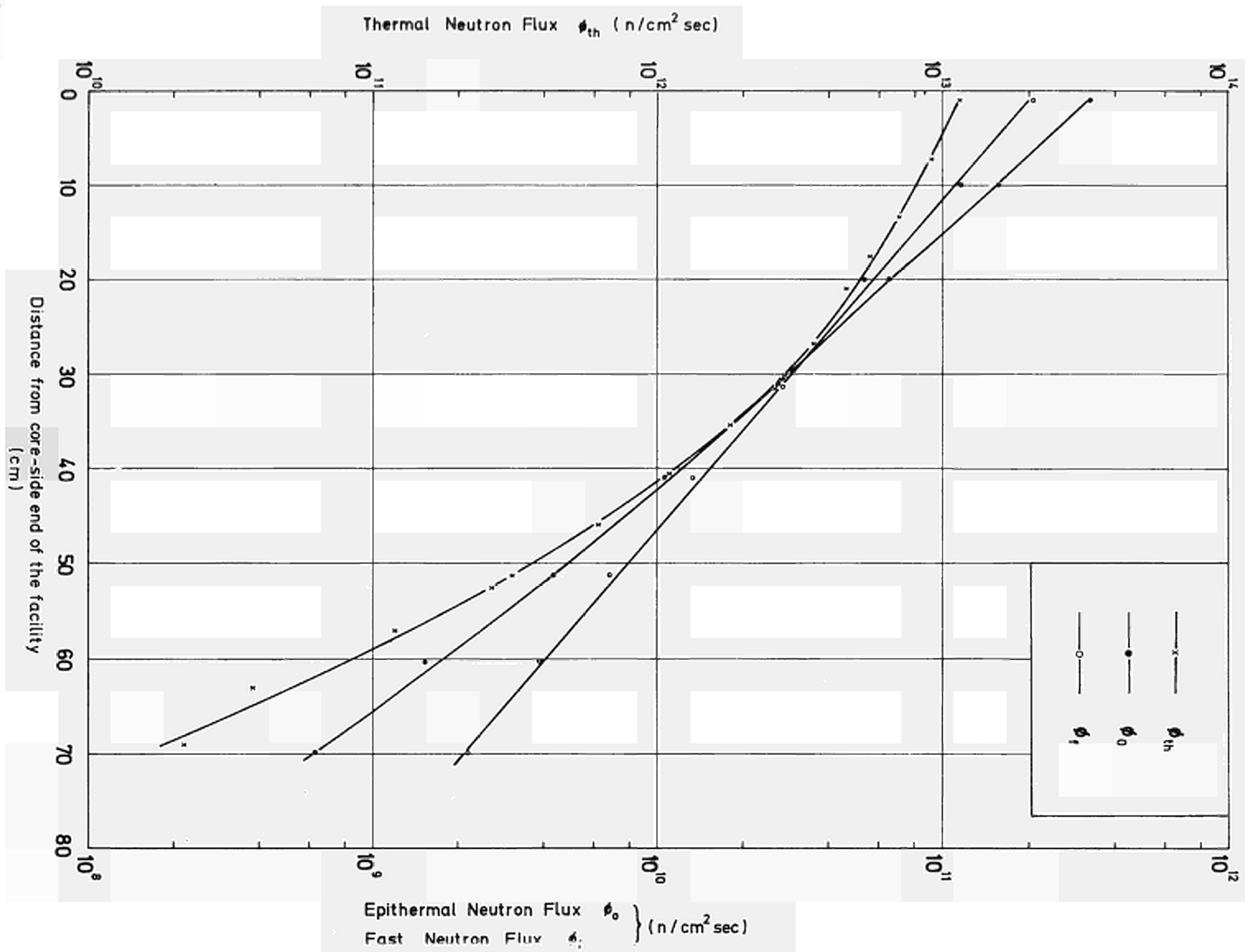
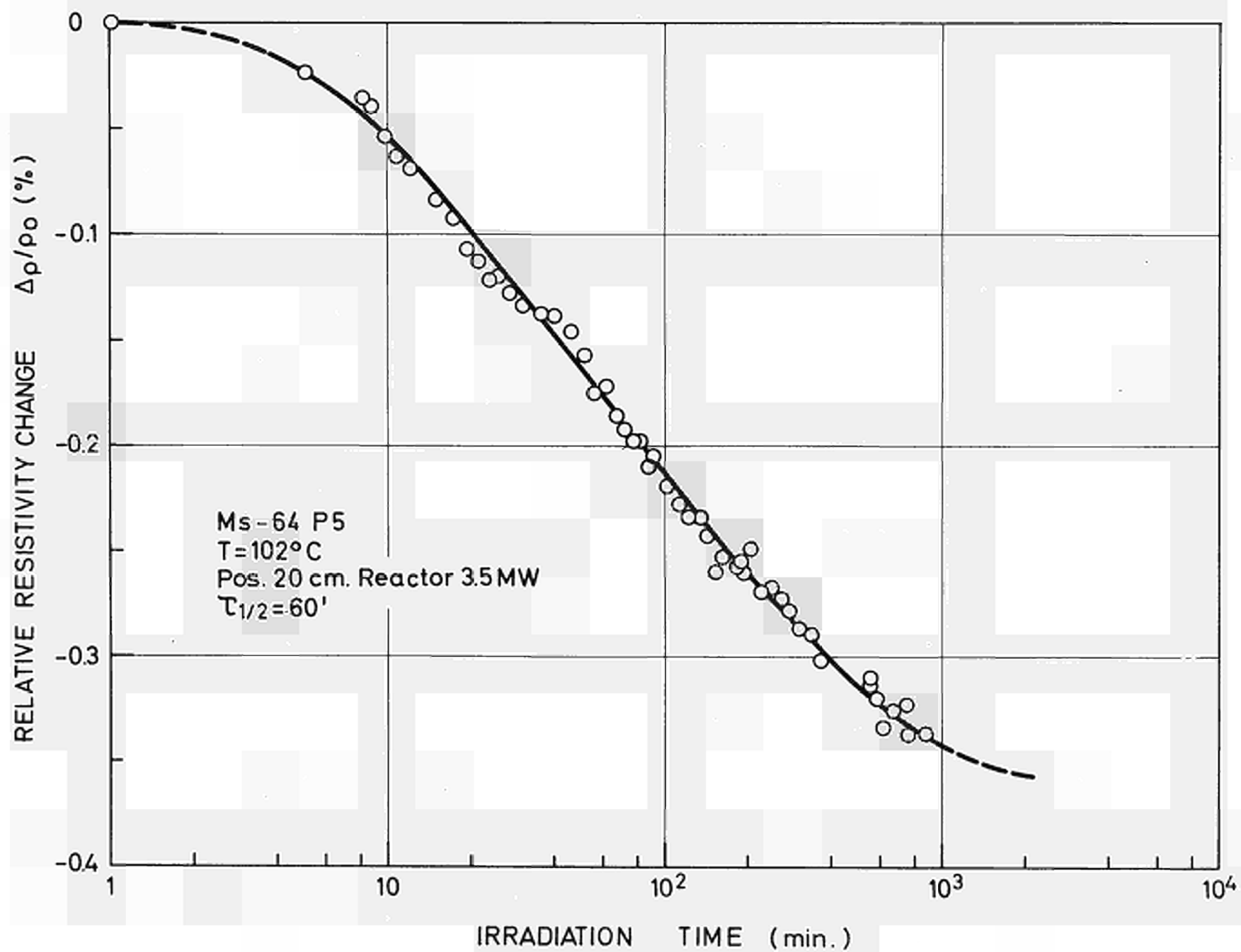


Figure 17

FIGURE 18



1

2

3

4

5

6

7

8

9

10

11

12

13

14

15

16

17

18

19

20

21

22

23

24

25

26

27

28

29

30

31

32

33

34

35

36

37

38

39

40



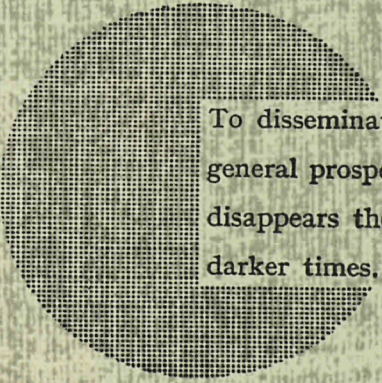
## NOTICE TO THE READER

All Euratom reports are announced, as and when they are issued, in the monthly periodical **EURATOM INFORMATION**, edited by the Centre for Information and Documentation (CID). For subscription (1 year : US\$ 15, £ 6.5) or free specimen copies please write to :

**Handelsblatt GmbH**  
**"Euratom Information"**  
**Postfach 1102**  
**D-4 Düsseldorf (Germany)**

or

**Office central de vente des publications**  
**des Communautés européennes**  
**2, Place de Metz**  
**Luxembourg**



To disseminate knowledge is to disseminate prosperity — I mean general prosperity and not individual riches — and with prosperity disappears the greater part of the evil which is our heritage from darker times.

Alfred Nobel

## SALES OFFICES

All Euratom reports are on sale at the offices listed below, at the prices given on the back of the front cover (when ordering, specify clearly the EUR number and the title of the report, which are shown on the front cover).

### OFFICE CENTRAL DE VENTE DES PUBLICATIONS DES COMMUNAUTES EUROPEENNES

2, place de Metz, Luxembourg (Compte chèque postal N° 191-90)

#### BELGIQUE — BELGIË

MONITEUR BELGE  
40-42, rue de Louvain - Bruxelles  
BELGISCH STAATSBLAD  
Leuvenseweg 40-42, - Brussel

#### LUXEMBOURG

OFFICE CENTRAL DE VENTE  
DES PUBLICATIONS DES  
COMMUNAUTES EUROPEENNES  
9, rue Goethe - Luxembourg

#### DEUTSCHLAND

BUNDESANZEIGER  
Postfach - Köln 1

#### NEDERLAND

STAATSDRUKKERIJ  
Christoffel Plantijnstraat - Den Haag

#### FRANCE

SERVICE DE VENTE EN FRANCE  
DES PUBLICATIONS DES  
COMMUNAUTES EUROPEENNES  
26, rue Desaix - Paris 15<sup>e</sup>

#### ITALIA

LIBRERIA DELLO STATO  
Piazza G. Verdi, 10 - Roma

#### UNITED KINGDOM

H. M. STATIONERY OFFICE  
P. O. Box 569 - London S.E.1

EURATOM — C.I.D.  
51-53, rue Belliard  
Bruxelles (Belgique)

CDNA04196ENC